© 2014. Published by The Company of Biologists Ltd | The Journal of Experimental Biology (2014) 217, 3146-3158 doi:10.1242/jeb.105437

RESEARCH ARTICLE

Thermal effects on the performance, motor control and muscle dynamics of ballistic feeding in the salamander *Eurycea guttolineata*

Christopher V. Anderson‡, Nicholas P. Larghi* and Stephen M. Deban

ABSTRACT

Temperature strongly affects muscle contractile rate properties and thus may influence whole-organism performance. Movements powered by elastic recoil, however, are known to be more thermally robust than muscle-powered movements. We examined the whole-organism performance, motor control and muscle contractile physiology underlying feeding in the salamander *Eurycea guttolineata*. We compared elastically powered tongue projection with the associated muscle-powered retraction to determine the thermal robustness of each of these functional levels. We found that tongue-projection distance in *E. guttolineata* was unaffected by temperature across the entire 4–26°C range, tongue-projection dynamics were significantly affected by temperature across only the 4–11°C interval, and tongue retraction was affected to a higher degree across the entire temperature range. The significant effect of temperature on projection dynamics across the 4–11°C interval corresponds to a significant decline in projector muscle burst intensity and peak contractile force of the projector muscle across the same interval. Across the remaining temperature range, however, projection dynamics were unaffected by temperature, with muscle contractile physiology showing typical thermal effects and motor patterns showing increased activity durations and latencies. These results reveal that elastically powered tongue-projection performance in *E. guttolineata* is maintained to a higher degree than muscle-powered tongue retraction performance across a wide temperature range. These results further indicate that thermal robustness of the elastically powered movement is dependent on motor control and muscle physiology that results in comparable energy being stored in elastic tissues across a range of temperatures.

KEY WORDS: Feeding, Tongue projection, Electromyography, Contractile properties, Temperature effects, Elastic

INTRODUCTION

The effect of temperature on movements powered by the recoil of elastic elements has been shown to be lower than the effect on associated movements powered directly by muscle contraction. Ballistic tongue-projection performance in chameleons, salamanders, toads and frogs, for instance, exhibits significantly lower thermal dependence than the performance of tongue retraction (Anderson and Deban, 2010; Deban and Lappin, 2011; Deban and Richardson, 2011; Sandusky and Deban, 2012). This pattern has been shown to be the result not of any compensatory activation of muscle at low temperature in chameleons and toads (Deban and Lappin, 2011; Anderson and Deban, 2012), nor of any unusually reduced effect of temperature on typical muscle contractile physiology in chameleons (Anderson and Deban, 2012). Instead, the specialized morphology and motor control patterns of these elastic recoil-powered tongue-projection mechanisms capitalize on the weak effect of temperature on muscle contractile force (Bennett, 1984; Herrel et al., 2007; Anderson and Deban, 2012; James, 2013) and the thermal independence of the mechanical properties of elastic tissues (Rigby et al., 1959; Alexander, 1966; Denny and Miller, 2006) to impart thermal robustness to these ballistic movements. Movements such as tongue retraction that are powered directly by muscle contraction, in contrast, suffer typical thermal effects resulting from the strong effect of temperature on muscle contractile dynamics, and thus slow significantly with decreasing temperature (Bennett, 1985; Rome, 1990; Herrel et al., 2007; Anderson and Deban, 2012; James, 2013). Thermal robustness of independently evolved ballistic movements powered by elastic recoil is well established; however, our understanding of the extent to which these mechanisms have converged on similar modifications to motor patterns, muscle contractile physiology or morphology to overcome strong thermal effects on muscle-powered movements remains limited. Here, we examined the thermal effects on the performance, motor control and muscle physiology of tongue projection in the plethodontid salamander *Eurycea guttolineata* (Holbrook 1838) to evaluate whether the motor control and muscle contractile patterns associated with thermal robustness in elastically powered movements in other taxa are also present in salamanders.

Tongue projection in plethodontid salamanders, including *E. guttolineata*, is extremely brief in duration, with the tongue reaching full extension in as little as 4 ms (Deban et al., 2007) (Fig. 1). The paired, cylindrical projector muscles, the m. subarcualis rectus (SAR), surround the elongated and tapered epibranchial cartilages of the tongue skeleton, which extend under the skin posteriorly over the shoulder from the buccal region. These cartilages are thrust forward by contraction of the muscle fibers of the SAR and recoil of the associated collagen fibers to carry the tongue from the mouth. The epibranchials articulate at their anterior ends with the paired ceratobranchials, which in turn connect medially with the unpaired basibranchial that supports the sticky tongue pad (Lombard and Wake, 1976; Wake and Deban, 2000). At maximal projection distances in *E. guttolineata*, the entire tongue skeleton is launched from the body as the epibranchials completely exit the center lumen of the SAR, and the tongue reaches the prey under its own momentum (Deban et al., 2007). The tongue is then retracted as the paired tongue-retractor muscles, the m. rectus cervicis profundus (RCP), which originate on the pelvis and insert into the tongue pad,

Department of Integrative Biology, University of South Florida, Tampa, FL 33620, USA.
*Present address: Florida Southern College, Lakeland, FL 33801, USA.

‡Author for correspondence at present address: Department of Ecology and Evolutionary Biology, Brown University, Providence, RI 02912, USA (Christopher_V_Anderson@brown.edu)

Received 18 March 2014; Accepted 17 June 2014

The Journal of Experimental Biology

The Journal of Experimental Biology (2014) doi:10.1242/jeb.105437

List of symbols and abbreviations

EMG	electromyography, electromyographic
P_0	peak isometric force
PRC	partial regression coefficients of the temperature effect
Q_{10}	temperature coefficient
RCP	m. rectus cervicis profundus
r.m.s.	root mean square
SAR	m. subarcualis rectus

contract to draw the tongue skeleton back to its resting position with the epibranchials inside the SAR muscles.

Electromyographic (EMG) recordings of muscle activity during feeding in plethodontid salamanders with ballistic tongue projection (*Hydromantes* and *Bolitoglossa*) have shown that, on the brief timescale of tongue projection, the SAR becomes active well before the tongue leaves the mouth (Deban and Dicke, 1999; Deban and Dicke, 2004; Deban et al., 2007), and this activity nearly ceases by the onset of tongue projection (Deban et al., 2007). This pattern indicates a phase in which the SAR myofibers contract and load collagenous elements of the muscle with potential energy that is subsequently released to power tongue launch. In these salamanders, as well as in *E. guttolineata*, the tongue is typically projected at performance levels that exceed the greatest maximum instantaneous power output of vertebrate muscle (Deban et al., 2007), implicating power amplification via elastic energy storage. These patterns are similar to tongue projection in chameleons (Wainwright and Bennett, 1992a; de Groot and van Leeuwen, 2004; Anderson and Deban, 2010; Anderson and Deban, 2012) and toads (Nishikawa, 2000; Lappin et al., 2006; Deban and Lappin, 2011), which, despite profound differences in morphology, also project their tongues with extreme performance and with activation of their projector muscles in advance of tongue projection.

The ballistic tongue-projection mechanism of *E. guttolineata* is independently evolved from that of chameleons, anurans and another plethodontid (*Hydromantes*) (Deban et al., 2007; Vieites et al., 2011) that has been shown to exhibit high-power tongue projection that is thermally robust (Deban and Richardson, 2011). The tongue morphology of *E. guttolineata* is, however, less extremely specialized for long-distance projection than that of *Hydromantes*; thus, the tongue-projection system of *Eurycea* provides a good opportunity to explore the generality of patterns of thermal robustness in elastically powered tongue projection and its underlying motor and muscle physiology. Given the similarity in the performance and basic mechanism of tongue projection in *E. guttolineata* to these other independently evolved systems, we predicted that thermal effects on the performance, motor control patterns and muscle contractile dynamics of tongue projection and retraction would also be similar. In particular, we hypothesized that, over a 5–25°C temperature range, tongue-projection distance and tongue-projection dynamics (e.g. velocity, power) would be

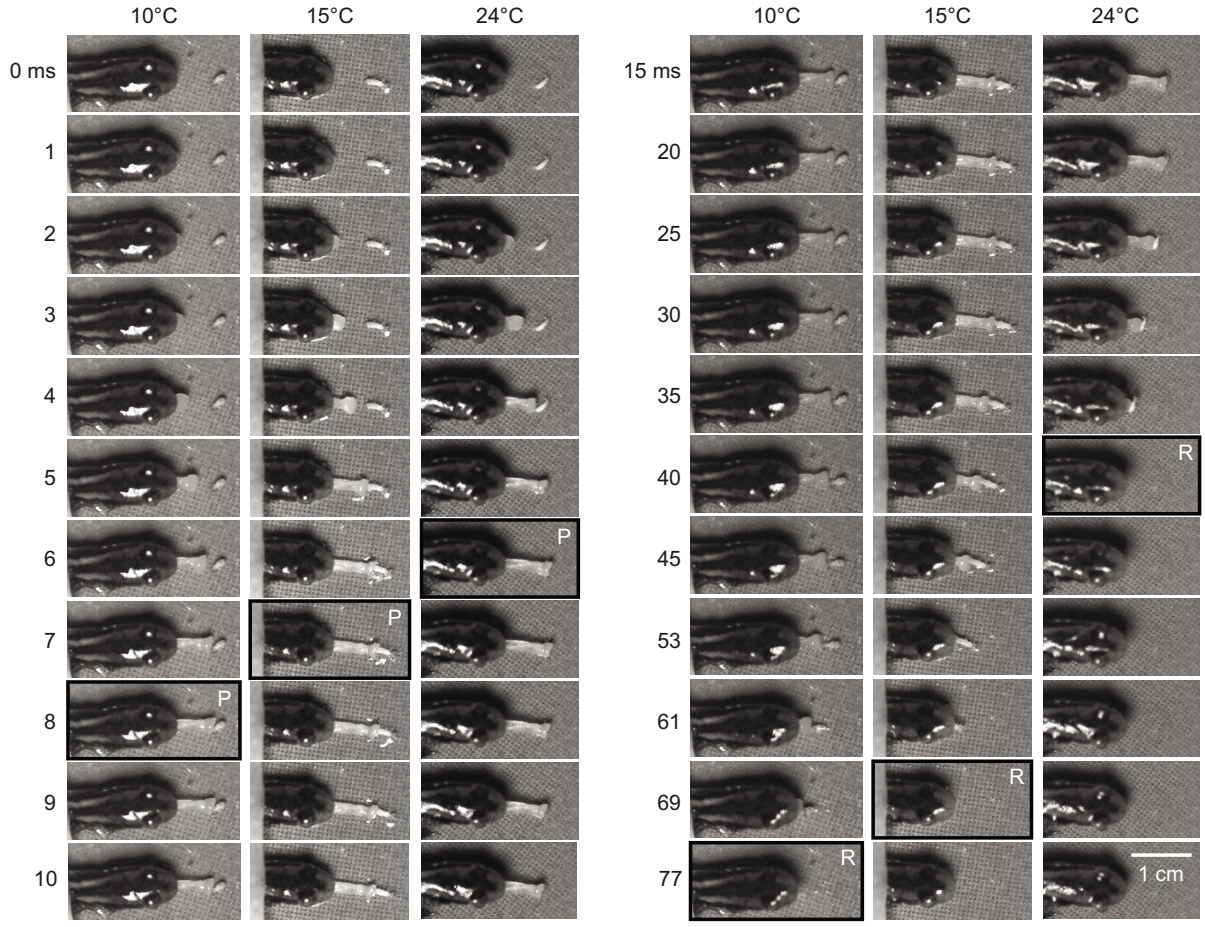

Fig. 1. Image sequences of an individual of *Eurycea guttolineata* feeding at 10, 15 and 24°C. The images show little difference in the duration of tongue projection (P indicates peak projection), yet pronounced differences in the duration of tongue retraction (ending at the frame marked R). Sequences begin at the start of tongue launch at time 0, progress downward from the top of the left column and continue at the top of the right column. The time step in the left column is 1 ms and 5–8 ms in the right column.

The Journal of Experimental Biology (2014) doi:10.1242/jeb.105437

unaffected or only weakly affected by temperature; however, tongue retraction dynamics (powered by muscle directly) would exhibit strong thermal effects. We also hypothesized that the intensity of muscle activity would not be affected by temperature – in particular, that it would not increase at low temperatures to compensate for reduced muscle contractile dynamics performance. Rather, we expected that, as has been observed in toads and chameleons, muscle activity duration would increase significantly at colder temperatures, with the projector muscle becoming active earlier relative to projection onset and the retractor muscle remaining active longer after projection onset. Finally, we expected that muscle contractile characteristics would be typical and hypothesized that static contractile properties (e.g. contractile tension) of both the projector and retractor muscles would exhibit weak temperature effects but that dynamic contractile properties (e.g. rate of tension development) would exhibit strong thermal effects.

RESULTS

Prey capture kinematics and dynamics

All *E. guttolineata* used tongue projection to capture prey during these experiments. Following orientation of the salamander toward the prey, the tongue was rapidly protracted from the mouth at tongue-projection distances of 0.16–1.21 cm (Table 1, Fig. 1, Fig. 2A). Upon contacting the tongue, the prey adhered to the salamander's sticky tongue pad. The prey was then drawn into the mouth along with the retracting tongue. The entire feeding event was performed rapidly in all cases, taking less than a second to complete even in the slowest events (Table 1, Fig. 1, Fig. 2B,C). Projection distance was not significantly affected by temperature across any of the temperature intervals, and, on average, both tongue projection and tongue retraction duration tended to increase with decreasing temperature across the entire temperature range (supplementary material Table S1; Fig. 1, Fig. 2A–C).

Salamanders were able to project the tongue and capture prey across the full range of experimental temperatures. A total of 154 feedings were recorded from 15 individuals across a 4.9–25.1°C temperature range (Table 1). Feedings collected from a single individual (eight feedings total) were excluded from dynamic analysis, because images of these feedings exhibited insufficient contrast to accurately digitize tongue position beyond determining the time of the start of tongue projection, the time of maximal tongue projection and the time of the end of tongue retraction.

Across the entire temperature range, salamanders achieved maximal tongue projection in 13±0.8 ms (mean ± s.e.m.), at an average velocity of 0.69±0.03 m s^{-1} (Table 1, Fig. 2B,C). Peak instantaneous projection velocities averaged 1.41±0.05 m s^{-1}, with peak instantaneous acceleration of 684±38 m s^{-2} and a peak instantaneous muscle mass-specific power of 788±60 W kg^{-1} (Table 1, Fig. 3A–C). All kinematic and dynamic variables for tongue projection significantly increased with increasing temperatures in the 4–11°C interval [temperature coefficient (Q_{10}) and $1/Q_{10}$>2], while none were significantly affected by temperature in any other temperature interval (supplementary material Table S1; Fig. 2B,C, Fig. 3A–C).

Tongue retraction was slower than projection, taking 50±6 ms for the tongue to completely retract into the mouth following maximal tongue projection, at an average velocity of 0.18±0.01 m s^{-1} over the entire temperature range (Table 1, Fig. 1, Fig. 2D,E). The tongue was retracted at peak instantaneous velocities of 0.31±0.01 m s^{-1} (Table 1, Fig. 3D). Peak instantaneous retraction accelerations averaged 30.2±2.3 m s^{-2} with peak instantaneous muscle mass-specific power averaging 8.3±0.9 W kg^{-1} (Table 1, Fig. 3E,F). All kinematic and dynamic variables for tongue retraction significantly increased with increasing temperature in the 4–11°C interval (Q_{10} and $1/Q_{10}$>2), while significance in other temperature intervals varied (supplementary material Table S1; Fig. 2D,E, Fig. 3D–F). Peak retraction velocity, for instance, significantly decreased with decreasing temperature in the 4–11, 9–16 and 19–26°C temperature intervals (Q_{10}>1.6) (supplementary material Table S1; Fig. 3D), while tongue retraction duration significantly increased and average retraction velocity significantly decreased at lower temperatures over the 4–11, 14–21 and 19–26°C temperature intervals (Q_{10} and $1/Q_{10}$>1.4) (supplementary material Table S1; Fig. 2D,E). Further, peak retraction acceleration and power significantly decreased with decreasing temperature in the 4–11 and 9–16°C intervals (Q_{10}>3.6) (supplementary material Table S1; Fig. 3E,F).

Motor control of prey capture

In all feeding events the SAR became active prior to the tongue exiting the mouth (Table 1, Fig. 4, Fig. 5B). This activity burst of the SAR ended either immediately before or after the tongue first became visible as it left the mouth. The RCP became active after the SAR, with its activity burst beginning either just before or sometime after the onset of tongue projection (Table 1, Fig. 4, Fig. 5E). The RCP was then active throughout the tongue retraction phase. Activity duration for both the SAR and RCP increased as temperature declined (supplementary material Table S2; Fig. 4, Fig. 5A,D). As temperature declined, the SAR became active earlier relative to tongue-projection onset while RCP activity extended longer after the onset of tongue projection (supplementary material Table S2; Fig. 4, Fig. 5B,D,E).

Of the 154 aforementioned feedings, a total of 151 feedings from 14 individuals from across the full temperature range had associated EMG recordings (Table 1). In feedings across the 4.9–25.1°C temperature range, the SAR was active for 144±5 ms, with the start of activity preceding the onset of tongue projection by 123±4 ms (Table 1, Fig. 5A,B). Activity duration of the SAR was significantly prolonged at lower temperatures across the 4–11 and 9–16°C temperature intervals, while across each temperature interval the latency between SAR activity onset and tongue-projection onset was significantly greater at lower temperatures ($1/Q_{10}$>1.5) (supplementary material Table S2; Fig. 4, Fig. 5A,B). Additionally, SAR root mean square (r.m.s.), SAR integrated area/duration, and SAR r.m.s. maximum amplitude were all significantly lower at lower temperatures across the 4–11°C interval (Q_{10}>3.75), while SAR r.m.s. and SAR r.m.s. maximum amplitude were significantly reduced at decreasing temperatures across the 14–21°C interval (Q_{10}>1.4) (supplementary material Table S2; Fig. 5C). SAR maximum amplitude to tongue-projection duration decreased significantly at lower temperatures over the 9–16°C interval ($1/Q_{10}$=3.12) but SAR activity cessation to tongue-projection onset was not significantly affected by temperature across any temperature interval (supplementary material Table S2).

Across the full 4.9–25.1°C temperature range, the RCP was active for 91±3 ms, with the start of activity averaging 1±2 ms before the onset of tongue projection (Table 1, Fig. 5C,D). Further, the onset of RCP activity averaged 14±2 ms before the time of maximum tongue projection, with peak RCP activity generally occurring 22±2 ms after the time of maximum tongue projection (Table 1). Only RCP activity duration across the 4–11°C interval was significantly affected by temperature ($1/Q_{10}$ value of 3.00), while no other motor control variables for the RCP, reflecting latency and excitation, were significantly affected by temperature (supplementary material Table S2; Fig. 4, Fig. 5D,E).

Table 1. Minimum and maximum values of kinematic, electromyographic and contractile variables in *Eurycea guttolineata*

	5±1°C		10±1°C		15±1°C		20±1°C		25±1°C	
Variables	Min./max.	Sample size	Min./max.	Sample size	Min./max.	Sample size	Min./max.	Sample size	Min./max.	Sample size
Kinematics and performance										
Projection distance (cm)	0.32/0.63	16 (7; 1–5)	0.25/0.96	31 (11; 1–5)	0.17/1.04	33 (11; 1–5)	0.16/1.15	47 (15; 1–8)	0.46/1.21	27 (9; 2–5)
Time of max. tongue projection (s)	0.009/0.068	16 (7; 1–5)	0.004/0.038	31 (11; 1–5)	0.005/0.039	33 (11; 1–5)	0.005/0.036	47 (15; 1–8)	0.005/0.016	27 (9; 2–5)
Time of completed tongue retraction (s)	0.084/0.177	16 (7; 1–5)	0.034/0.118	31 (11; 1–5)	0.021/0.873	33 (11; 1–5)	0.019/0.076	47 (15; 1–8)	0.024/0.065	27 (9; 2–5)
Peak projection velocity (m s^{-1})	0.32/1.58	16 (7; 1–5)	0.51/2.18	29 (10; 1–5)	0.36/2.06	30 (10; 1–5)	0.38/2.60	44 (14; 1–8)	0.86/3.03	27 (9; 2–5)
Average projection velocity (m s^{-1})	0.07/0.64	16 (7; 1–5)	0.12/1.37	31 (11; 1–5)	0.07/1.12	33 (11; 1–5)	0.09/1.41	47 (15; 1–8)	0.43/1.46	27 (9; 2–5)
Peak projection acceleration (m s^{-2})	61/551	16 (7; 1–5)	89/1180	29 (10; 1–5)	129/1410	30 (10; 1–5)	101/1700	44 (14; 1–8)	245/3510	27 (9; 2–5)
Peak projection mass-specific power (W kg^{-1})	17/613	16 (7; 1–5)	30/2155	29 (10; 1–5)	36/2075	30 (10; 1–5)	31/3311	44 (14; 1–8)	170/4742	27 (9; 2–5)
Max. projection kinetic energy (J)	1.34×10^{-6}/ 3.33×10^{-5}	16 (7; 1–5)	3.48×10^{-6}/ 6.34×10^{-5}	29 (10; 1–5)	1.72×10^{-6}/ 5.66×10^{-5}	30 (10; 1–5)	1.96×10^{-6}/ 9.01×10^{-5}	44 (14; 1–8)	9.91×10^{-6}/ 1.22×10^{-4}	27 (9; 2–5)
Max. projection kinetic energy (J kg^{-1} muscle mass)	0.06/1.42	16 (7; 1–5)	0.15/2.71	29 (10; 1–5)	0.07/2.42	30 (10; 1–5)	0.08/3.85	44 (14; 1–8)	0.42/2.14	27 (9; 2–5)
Peak retraction velocity (m s^{-1})	0.07/0.24	16 (7; 1–5)	0.09/0.56	29 (10; 1–5)	0.13/0.60	30 (10; 1–5)	0.13/0.79	44 (14; 1–8)	0.26/0.81	27 (9; 2–5)
Average retraction velocity (m s^{-1})	0.04/0.10	16 (7; 1–5)	0.04/0.25	31 (11; 1–5)	0.01/0.27	33 (11; 1–5)	0.04/0.47	47 (15; 1–8)	0.11/0.54	27 (9; 2–5)
Peak retraction acceleration (m s^{-2})	2.1/16.2	16 (7; 1–5)	4.0/43.1	29 (10; 1–5)	3.9/101.0	30 (10; 1–5)	4.4/171.0	44 (14; 1–8)	1.5/144.0	27 (9; 2–5)
Peak retraction mass-specific power (W kg^{-1})	0.10/2.84	16 (7; 1–5)	0.26/10.50	29 (10; 1–5)	0.38/38.76	30 (10; 1–5)	1.19/74.16	44 (14; 1–8)	0.37/65.16	27 (9; 2–5)
Muscle activity (s)										
SAR activity duration	0.133/0.387	16 (7; 1–5)	0.095/0.318	31 (11; 1–5)	0.083/0.226	33 (11; 1–5)	0.062/0.166	44 (14; 1–8)	0.062/0.145	27 (9; 2–5)
SAR onset to tongue projection onset duration	0.148/0.279	16 (7; 1–5)	0.120/0.237	31 (11; 1–5)	0.084/0.184	33 (11; 1–5)	0.068/0.155	44 (14; 1–8)	0.063/0.095	27 (9; 2–5)
SAR max. amplitude to tongue projection duration	0.026/0.213	16 (7; 1–5)	0.022/0.226	31 (11; 1–5)	0.009/0.162	33 (11; 1–5)	–0.005/ 0.133	44 (14; 1–8)	0.012/0.071	27 (9; 2–5)
SAR offset to tongue projection onset duration	–0.116/ 0.068	16 (7; 1–5)	–0.109/ 0.031	31 (11; 1–5)	–0.123/ 0.018	33 (11; 1–5)	–0.066/ 0.018	44 (14; 1–8)	–0.071/ 0.006	27 (9; 2–5)
RCP activity duration	0.071/0.240	16 (7; 1–5)	0.047/0.237	31 (11; 1–5)	0.031/0.187	33 (11; 1–5)	0.025/0.171	44 (14; 1–8)	0.043/0.145	27 (9; 2–5)
RCP onset to tongue projection duration	–0.024/ 0.057	16 (7; 1–5)	–0.050/ 0.167	31 (11; 1–5)	–0.121/ 0.035	33 (11; 1–5)	–0.048/ 0.063	44 (14; 1–8)	–0.019/ 0.066	27 (9; 2–5)
RCP onset to max. tongue projection duration	0.002/0.125	16 (7; 1–5)	– 0.040/ 0.178	31 (11; 1–5)	–0.089/ 0.055	33 (11; 1–5)	–0.042/ 0.078	44 (14; 1–8)	–0.003/ 0.073	27 (9; 2–5)
RCP max. amplitude to max. projection duration	–0.071/ 0.029	16 (7; 1–5)	–0.090/ 0.121	31 (11; 1–5)	–0.145/ 0.014	33 (11; 1–5)	–0.091/ 0.007	44 (14; 1–8)	–0.065/ 0.001	27 (9; 2–5)
Contractile variables										
SAR P_0 (N)	0.04/0.11	14 (6; 2–3)	0.04/0.13	14 (6; 2–3)	0.04/0.19	25 (6; 4–5)	0.04/0.17	13 (6; 2–3)	0.05/0.18	12 (6; 2–2)
SAR time to 90% P_0 (s)	0.186/0.309	14 (6; 2–3)	0.144/0.243	14 (6; 2–3)	0.118/0.181	25 (6; 4–5)	0.114/0.188	13 (6; 2–3)	0.094/0.145	12 (6; 2–2)
SAR rate of force development (N s^{-1})	0.17/0.64	14 (6; 2–3)	0.23/1.05	14 (6; 2–3)	0.32/1.85	25 (6; 4–5)	0.33/2.82	13 (6; 2–3)	0.51/3.38	12 (6; 2–2)
SAR electromechanical delay (s)	0.013/0.031	14 (6; 2–3)	0.007/0.017	14 (6; 2–3)	0.005/0.023	25 (6; 4–5)	0.005/0.010	13 (6; 2–3)	0.004/0.007	12 (6; 2–2)
RCP P_0 (N)	0.02/0.07	12 (6; 2–2)	0.03/0.09	12 (6; 2–2)	0.02/0.09	25 (6; 4–5)	0.04/0.11	12 (6; 2–2)	0.02/0.10	12 (6; 2–2)
RCP time to 90% P_0 (s)	0.135/0.177	12 (6; 2–2)	0.105/0.131	12 (6; 2–2)	0.089/0.120	25 (6; 4–5)	0.082/0.098	12 (6; 2–2)	0.076/0.093	12 (6; 2–2)
RCP rate of force development (N s^{-1})	0.16/1.04	12 (6; 2–2)	0.56/2.11	12 (6; 2–2)	0.56/3.26	25 (6; 4–5)	1.42/4.73	12 (6; 2–2)	1.04/5.08	12 (6; 2–2)
RCP electromechanical delay (s)	0.012/0.034	12 (6; 2–2)	0.008/0.021	12 (6; 2–2)	0.004/0.017	25 (6; 4–5)	0.005/0.007	12 (6; 2–2)	0.004/0.005	12 (6; 2–2)
RCP specific tension (N cm^{-2})	3.83/16.47	12 (6; 2–2)	6.94/18.11	12 (6; 2–2)	5.03/22.44	25 (6; 4–5)	8.86/21.93	12 (6; 2–2)	5.63/21.99	12 (6; 2–2)

RCP, m. rectus cervicis; SAR, m. subarcualis rectus; P_0, peak isometric force.

The total number of feedings (for kinematic and electromyographic variables) or contractions (for contractile variables) is presented for each variable as well as the number of individuals data was gathered from and the range of feedings for each individual (in parentheses separated by a semicolon) in the sample size columns.

The Journal of Experimental Biology (2014) doi:10.1242/jeb.105437

The Journal of Experimental Biology (2014) doi:10.1242/jeb.105437

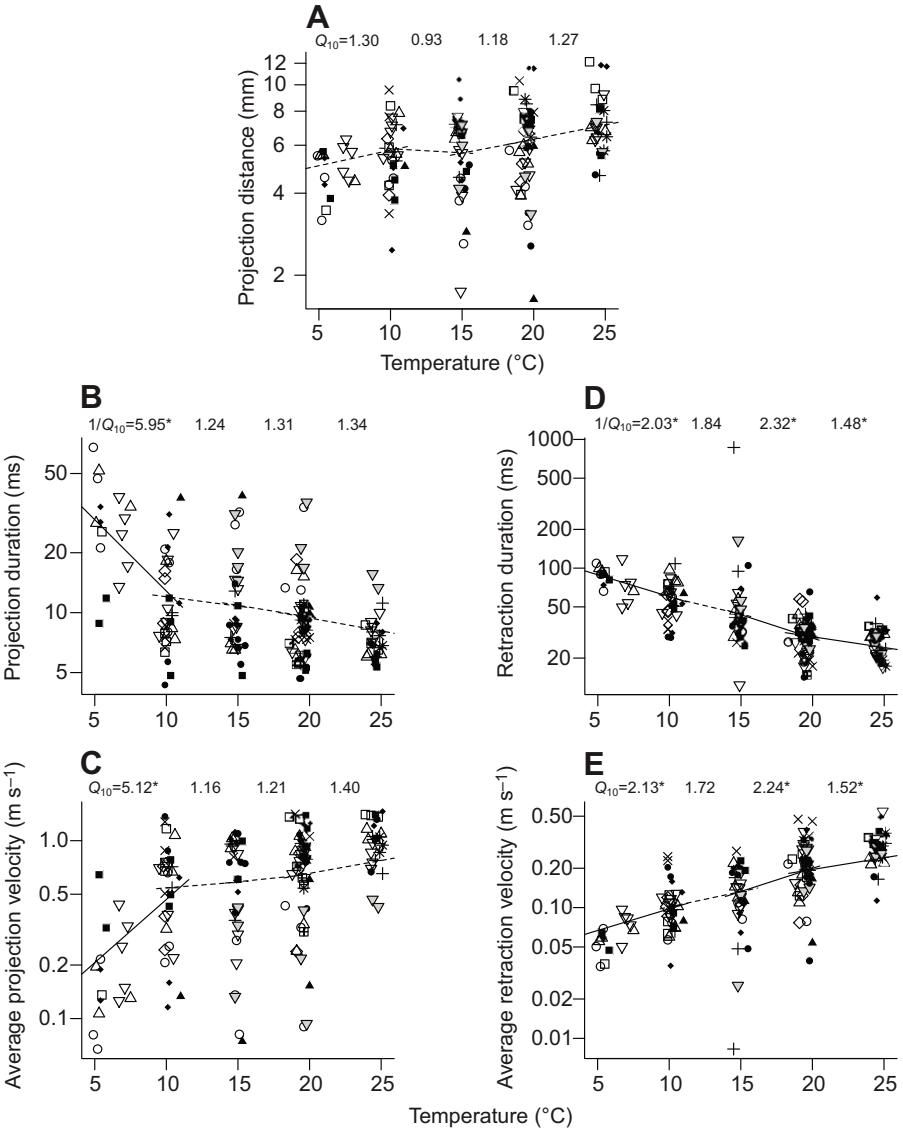

Fig. 2. Scatterplots of kinematic variables from all feedings for each variable versus temperature. (A) Overall maximal tongue-projection distance; (B,C) variables for tongue projection; (D,E) variables for tongue retraction. Regressions representing Q_{10} values are derived from the partial regression coefficients of the temperature effect in the ANCOVA (see Materials and methods for details), which are shown as lines overlaid on the data points across the 4–11, 9–16, 14–21 and 19–26°C intervals. Tongue-projection distance (A) depicts only non-significant effects of temperature across each temperature range, while the remaining tongue-projection variables (B,C) depict significant effects only across the 4–11°C interval, and tongue retraction variables (D,E) depict significant effects across each temperature interval except the 9–16°C interval (see supplementary material Table S1 for details). A significant temperature effect is depicted as a solid regression line and indicated by an asterisk, whereas non-significant temperature effects are depicted as dashed regression lines. Note that the *y*-axes have log scales and therefore depict the exponential relationships between the variables and temperature as straight lines. Individual salamanders are shown as different symbols.

Muscle contractile dynamics

For both the SAR and RCP, force increased after a brief delay following the onset of stimulation, reached its maximum within about 300 ms and then formed a force plateau characteristic of fused tetanus (Table 1). Force declined rapidly after a brief delay following the end of stimulation. Peak force increased with temperature for the SAR across the entire temperature range, while peak force for the RCP increased with increasing temperature across each temperature interval with the exception of 19–26°C (supplementary material Table S3; Fig. 6C,F). Latencies between stimulation and force production, as well as rates of force production for both muscles showed that the muscles slowed with decreasing temperature across the entire temperature range (supplementary material Table S3; Fig. 6A,B,D,E).

Over the entire 4–26°C temperature interval, the SAR produced a peak isometric force (P_0) of 0.08±0.004 N (Table 1, Fig. 6C) from paired tubular muscles of 0.017–0.034 g combined mass. Following a 10.3±0.6 ms electromechanical delay, these contractions reached 90% P_0 in 105±5 ms at a rate of 0.88±0.07 N s^{-1} (Table 1, Fig. 6A,B). Across the 4–11°C interval, P_0 was significantly greater at higher temperatures (Q_{10}=1.23), while it was not affected by temperature across the remaining temperature intervals (supplementary material Table S3; Fig. 6C). The rate of force development was significantly higher at higher temperatures across the 4–11, 9–16 and 19–26°C intervals (Q_{10}>1.75) but not across the 14–21°C interval (supplementary material Table S3; Fig. 6B). The time to 90% P_0 and the electromechanical delay both declined significantly with increasing temperature across all temperature intervals (1/Q_{10}>1.3) (supplementary material Table S3; Fig. 6A).

Across the 4–26°C interval, the RCP reached a P_0 of 0.07±0.003 N (Table 1; Fig. 6F) from paired linear muscle segments of 0.010–0.016 g combined mass, with a specific tension of 14.12±0.56 N cm^{-2}. These contractions reached 90% P_0 in 42±2 ms at a rate of 1.78±0.13 N s^{-1} following a 9.8±0.7 ms electromechanical delay (Table 1; Fig. 6D,E). With the exception of the rate of force development across the 19–26°C interval, all contractile properties of the RCP were significantly affected by temperature across each temperature range (supplementary material Table S3; Fig. 6D–F). Across the 4–11, 9–16 and 14–21°C interval, P_0 increased with temperature (Q_{10}>1.1), while across the 19–26°C interval, P_0 declined (Q_{10}=0.81) (supplementary material Table S3; Fig. 6F). All duration variables for RCP contractions that were significantly affected by temperature decreased with increasing temperature, while the rate of force development increased with

The Journal of Experimental Biology (2014) doi:10.1242/jeb.105437

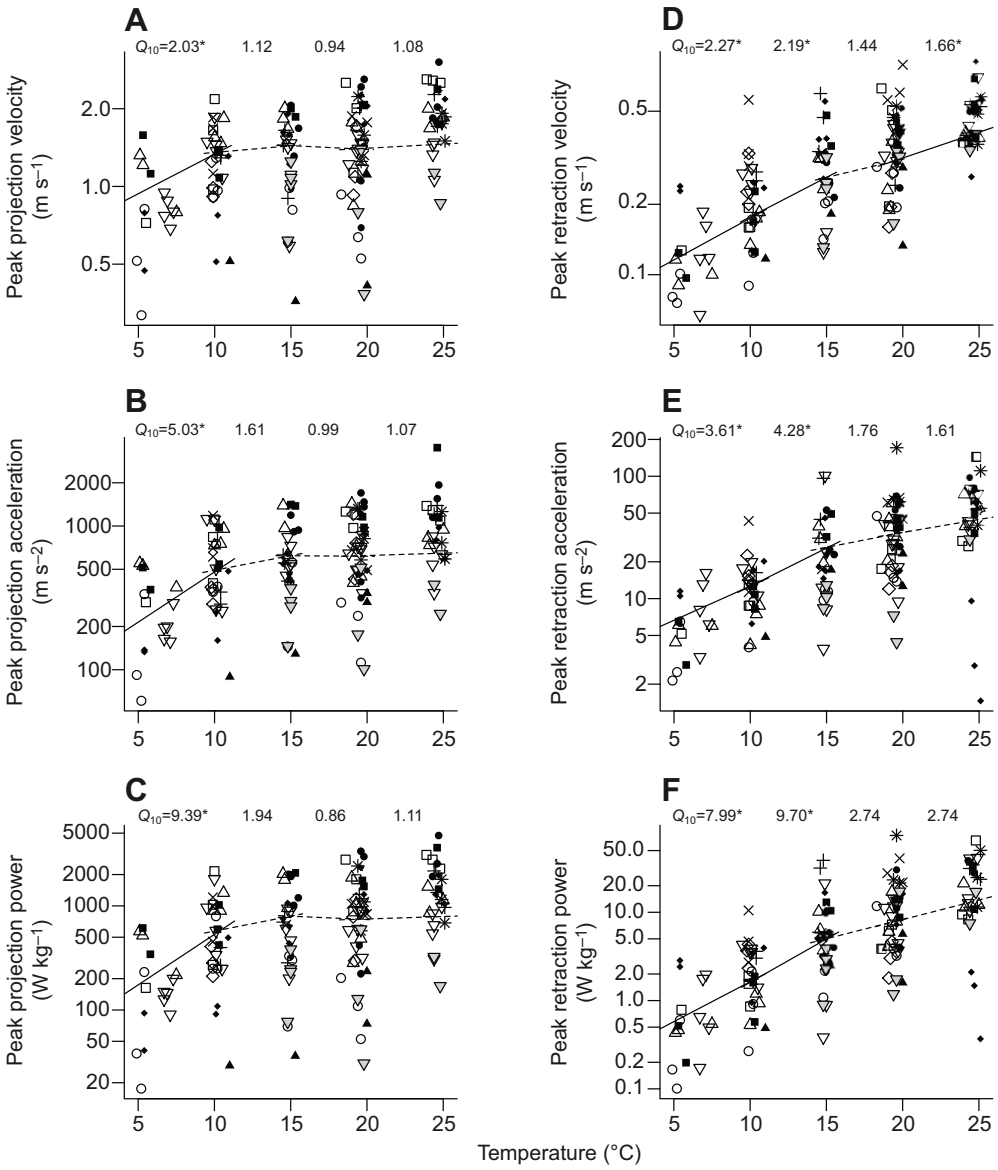

Fig. 3. Scatterplots of peak dynamic variables versus temperature. (A–C) Variables for tongue projection; (D–F) variables for tongue retraction. A significant effect of temperature is depicted for tongue-projection variables (A–C) across only the 4–11°C interval for each variable, while for tongue retraction (D–F), a significant effect is revealed across both the 4–11 and 9–16°C interval for each variable and the 19–26°C interval for peak retraction velocity (D; see supplementary material Table S1 for details). Indications as in Fig. 2.

increasing temperature across each interval (Q_{10} and $1/Q_{10}$>1.75) (supplementary material Table S3; Fig. 6D,E).

DISCUSSION

Prey capture kinematics and dynamics

As previously shown in some plethodontid salamander species, the *E. guttolineata* in this study captured prey by tongue projection, in which the tongue pad and tongue skeleton are projected out of the mouth, traveling to the prey under their own momentum in more distant feedings (Fig. 1) (Deban et al., 1997; Deban and Dicke, 1999; Deban and Dicke, 2004; Deban et al., 2007; Deban and Richardson, 2011). Tongue-projection performance values overlapped with those previously measured for *Eurycea* over a much narrower range of temperatures (22–24°C) (Deban et al., 2007). The range in performance observed in this study suggests these salamanders have the ability to modulate their performance levels to a high degree. The majority of instantaneous muscle mass-specific power output values for tongue projection (mean ± s.e.m. 788±60 W kg^{-1}), however, exceeded the maximum muscle power estimated for amphibians (373 W kg^{-1} at 25°C) (Lutz and Rome, 1994). This indicates that *Eurycea* uses an elastic-recoil mechanism to enhance power output, which is also consistent with previous results (Deban et al., 2007). Despite this modulatory ability and the fact that various aspects of feeding were strongly affected by temperature (supplementary material Tables S1–S3; Figs 1–6), the salamanders in this study were capable of ballistic tongue projection at all temperatures (4.9–25.1°C), and tongue-projection distance was unaffected by temperature (supplementary material Table S1; Fig. 2A).

In another plethodontid salamander (*Hydromantes*), and in frogs, toads and chameleons, elastic-recoil-powered tongue projection was weakly affected by temperature across all examined temperature intervals, while muscle-powered tongue retraction was strongly affected by temperature (Anderson and Deban, 2010; Deban and Lappin, 2011; Deban and Richardson, 2011; Sandusky and Deban, 2012). Patterns of thermal effects on the kinematics and dynamics of movements of *Eurycea* in this study, however, varied across the temperature ranges and between movement types. In the lowest temperature interval (4–11°C), for instance, both tongue projection and retraction movements were strongly affected by temperature, with projection being affected to a greater degree than retraction (supplementary material Table S1; Figs 1–3). Tongue projection was

The Journal of Experimental Biology (2014) doi:10.1242/jeb.105437

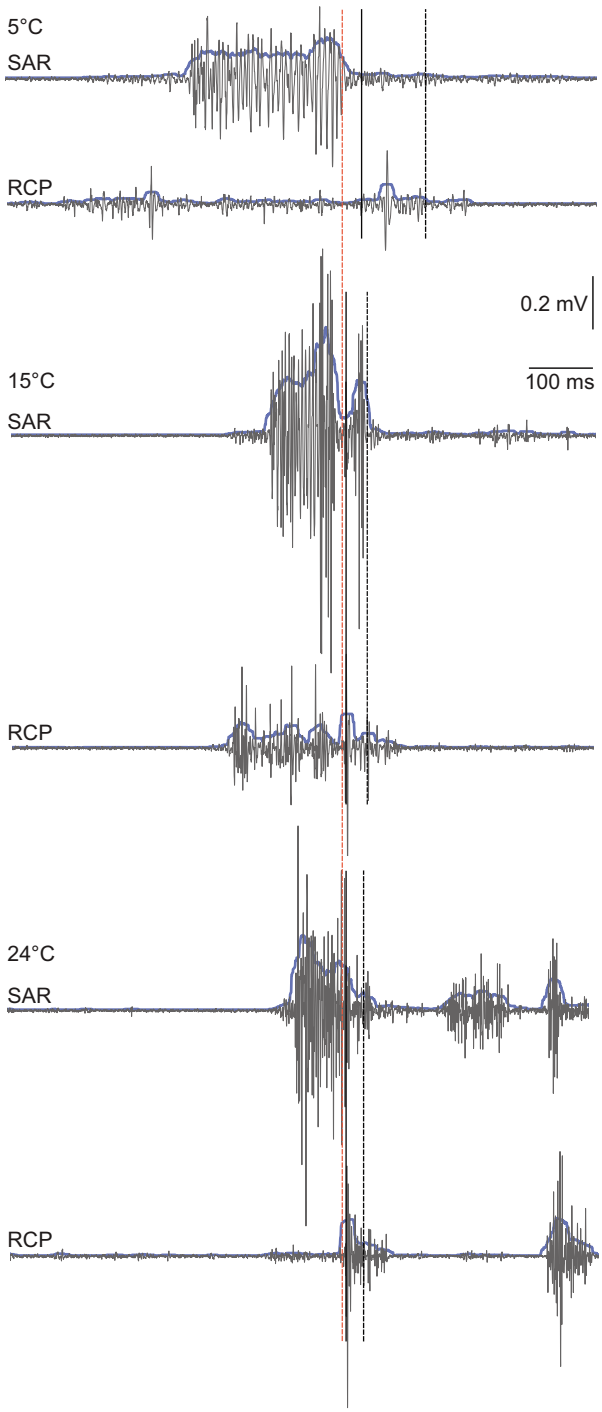

Fig. 4. Representative electromyographic (EMG) signals and the root mean square (r.m.s.) of the signals (20 ms time constant, blue lines) from the m. subarcualis rectus (SAR) and m. rectus cervicis profundus (RCP) in the same individual of *E. guttolineata* feeding at 5°C (top), 15°C (middle) and 24°C (bottom). Tongue-projection distance is similar (~6 mm) in all feedings. Traces are aligned at the onset of tongue projection (red vertical line extending through all traces). Time of maximal tongue projection is depicted by the solid vertical black line through traces of a given temperature and the time of full tongue retraction is depicted by the dashed vertical black line. Note the activation of the SAR prior to tongue projection and the extended activation of the SAR prior to tongue projection at lower temperatures compared with higher temperatures. Additionally, note the reduced SAR burst intensity and increased RCP activity duration at lower temperatures. Activity bursts associated with prey transport following tongue retraction are also depicted in traces at 24°C. Indicated scales apply to all traces.

not affected by temperature across the three higher temperature intervals (9–16, 14–21 and 19–26°C), while tongue retraction exhibited significant effects of temperature on varying performance parameters, with temperature coefficient values that tended to exceed those of ballistic movements across the same temperature intervals. Because the thermal effects on the mechanical properties of elastic structures, such as collagen aponeuroses, do not vary significantly across the examined temperature range, the strong thermal effects on elastically powered projection movements across the 4–11°C interval are likely the result of greater thermal effects on either the motor control or muscle contractile physiology underlying these movements. In fact, across the 4–11°C interval, muscle activity burst intensity and peak tetanic tension of the tongue-projector muscle declined significantly at lower temperatures (supplementary material Tables S2, S3; Table 1, Fig. 5C, Fig. 6C), both of which would result in lower elastic energy stored in collagenous tissues to power tongue projection at 4°C.

The results obtained from *E. guttolineata* are consistent with the hypotheses that tongue projection in this species is powered at least in part by an elastic-recoil mechanism, exhibiting reduced thermal sensitivity when compared with tongue retraction powered by muscle contraction directly. This dichotomy has been found in a number of integrated systems that incorporate an elastic-recoil-powered movement with an associated muscle-powered movement (Anderson and Deban, 2010; Deban and Lappin, 2011, Deban and Richardson, 2011; Sandusky and Deban, 2012, Anderson and Deban, 2012; Higham and Anderson, 2014) and is indicative of these elastic-recoil-powered mechanisms capitalizing on the weak effect of temperature on muscle contractile force and muscle work during near-isometric contractions (Bennett, 1984; Herrel et al., 2007; Anderson and Deban, 2012; James, 2013) as well as the thermal independence of elastic tissue mechanical properties (Rigby et al., 1959; Alexander, 1966; Denny and Miller, 2006) to impart thermal robustness to these ballistic movements. The strong thermal sensitivity of the elastic-recoil-powered movement in this study in the 4–11°C interval, however, emphasizes that this thermal robustness is contingent on relatively similar amounts of elastic energy being stored in the tongue's elastic elements by the tongue-projector muscles, by way of increased motor activity durations, equal burst intensity and similar tension development as temperature declines, as found previously in other systems (Deban and Lappin, 2011; Anderson and Deban, 2012). The plethodontid *Hydromantes platycephalus* is able to maintain high-performance tongue projection as low as 2°C (Deban and Richardson, 2011), suggesting that it maintains muscle activity and tension at lower temperatures than *E. guttolineata*, although thermal effects on its motor and muscle physiology have not been examined.

Motor control of prey capture

The activation patterns of the SAR in *E. guttolineata* accord with a pattern of muscle activation prior to tongue projection found in previous studies of other plethodontid species (Deban and Dicke, 2004; Deban et al., 2007) (Table 1, Fig. 4, Fig. 5A–C), during which time the SAR loads elastic structures with strain energy; these structures later recoil to power the majority of tongue projection. The onset of SAR activity occurred on average 123 ms prior to the onset of tongue projection, which was 9.5 times the average time for the tongue to reach maximum projection and sufficient time for the SAR to load elastic structures with strain energy. While SAR activity occasionally extended beyond the onset of tongue projection, activity beginning no less than 63 ms prior to the onset of tongue projection is consistent with a 'bow and arrow'

The Journal of Experimental Biology (2014) doi:10.1242/jeb.105437

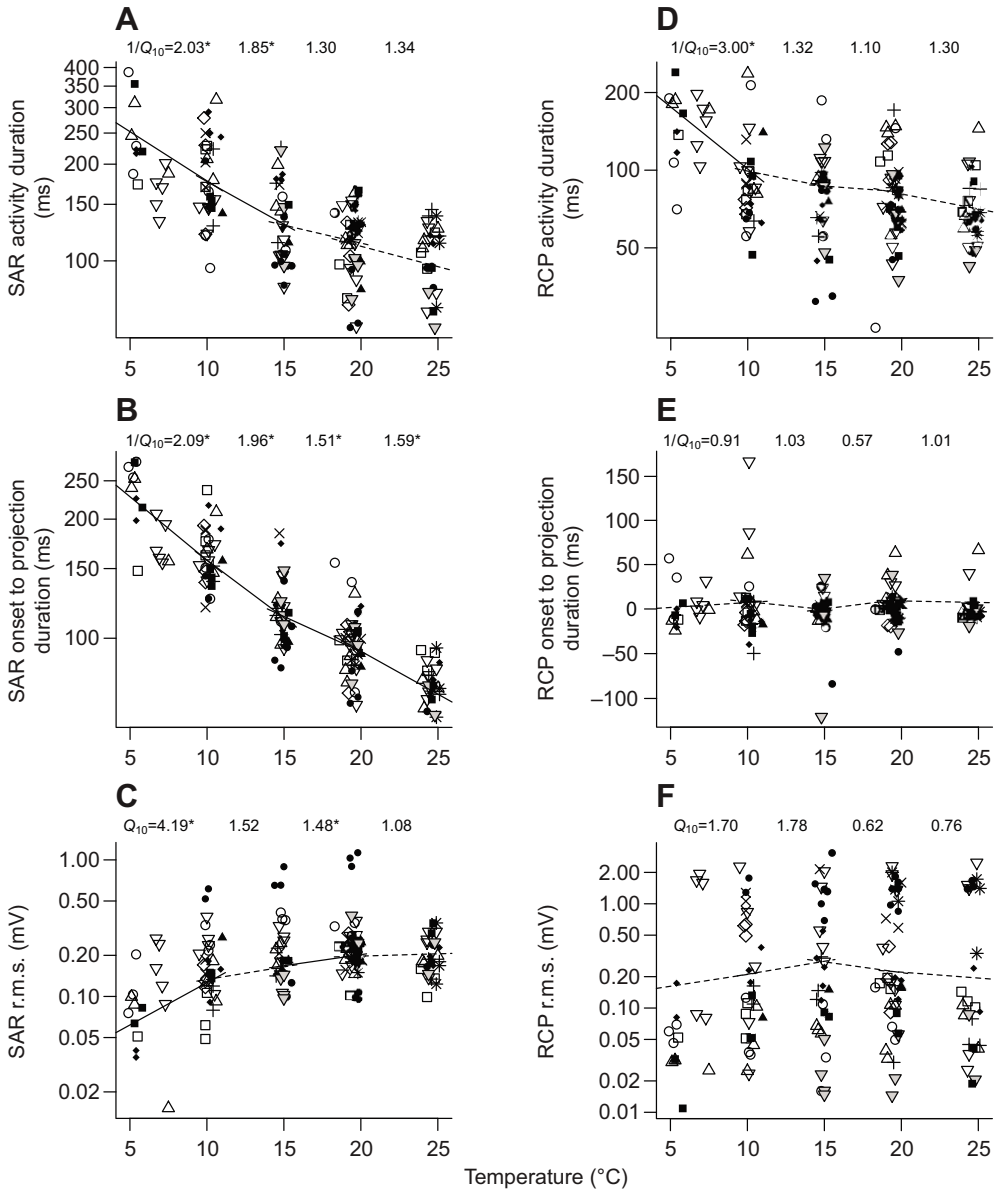

Fig. 5. Scatterplots of EMG variables versus temperature. (A–C) Variables for the SAR; (D–F) variables for the RCP. Significant temperature effects for SAR variables are depicted across the 4–11 and 9–16°C intervals for SAR activity duration (A), across each temperature interval for SAR onset to projection onset duration (B), and across the 4–11 and 14–21°C intervals for SAR r.m.s. (C). A significant temperature effect for RCP variables, in contrast, is only depicted for RCP activity duration across the 4–11°C interval (D; see supplementary material Table S2 for details). Indications as in Fig. 2.

mechanism of loading and recoil of elastic structures. The continuation of SAR activity during tongue projection in some feedings suggests that the movement is not entirely elastically powered in those feedings and that active muscle contraction during tongue launch contributes to projection. A similar mechanism has been found in jumping frogs, in which both muscle shortening and elastic recoil occur during launch (Roberts and Marsh, 2003; Astley and Roberts, 2012). The activation of muscles well in advance of high-powered movements is a common phenomenon, having been found or implicated not only in salamanders (Deban and Dicke, 2004; Deban et al., 2007) but also in other high-powered movements in both vertebrates and invertebrates (Wainwright and Bennett, 1992a; Wainwright and Bennett, 1992b; de Groot and van Leeuwen, 2004; Patek et al., 2004; Burrows, 2006; Patek et al., 2006; Van Wassenbergh et al., 2008; Patek et al., 2007; Burrows, 2009; Anderson and Deban, 2010; Deban and Lappin, 2011; Roberts and Azizi, 2011; Anderson and Deban, 2012; Sandusky and Deban, 2012; Anderson and Higham, 2014; Higham and Anderson, 2014).

Temperature effects on the timing of activity of the SAR indicate that, as predicted, the SAR took significantly longer to load the tongue-projection mechanism as temperature declined. The lack of significant changes in the duration of activity or in the latency of maximal activity to projection onset at higher temperatures suggests that temperature effects are greater in the lower temperature intervals. These patterns of larger temperature effects at low temperature and increased loading time for the muscle associated with tongue projection are similar to those found during feeding in the jaw muscles of toads (Deban and Lappin, 2011) and in the tongue-projector muscle in chameleons (Anderson and Deban, 2012). These increasing temperature effects at low temperature likely reflect increased deviation from the thermal performance optima (Huey and Stevenson, 1979). Increased muscle activity durations (and presumably elastic loading times) relate to an increased duration required for the muscle to perform similar work on the elastic elements at slower contractile velocities and rates of force development (Vogel, 2003).

Activity patterns of the RCP are consistent with a pattern of braking tongue movement at the end of tongue projection and retracting the tongue into the mouth (Table 1, Fig. 4, Fig. 5D–F). Activity began on average 1.4 ms prior to the onset of tongue

The Journal of Experimental Biology (2014) doi:10.1242/jeb.105437

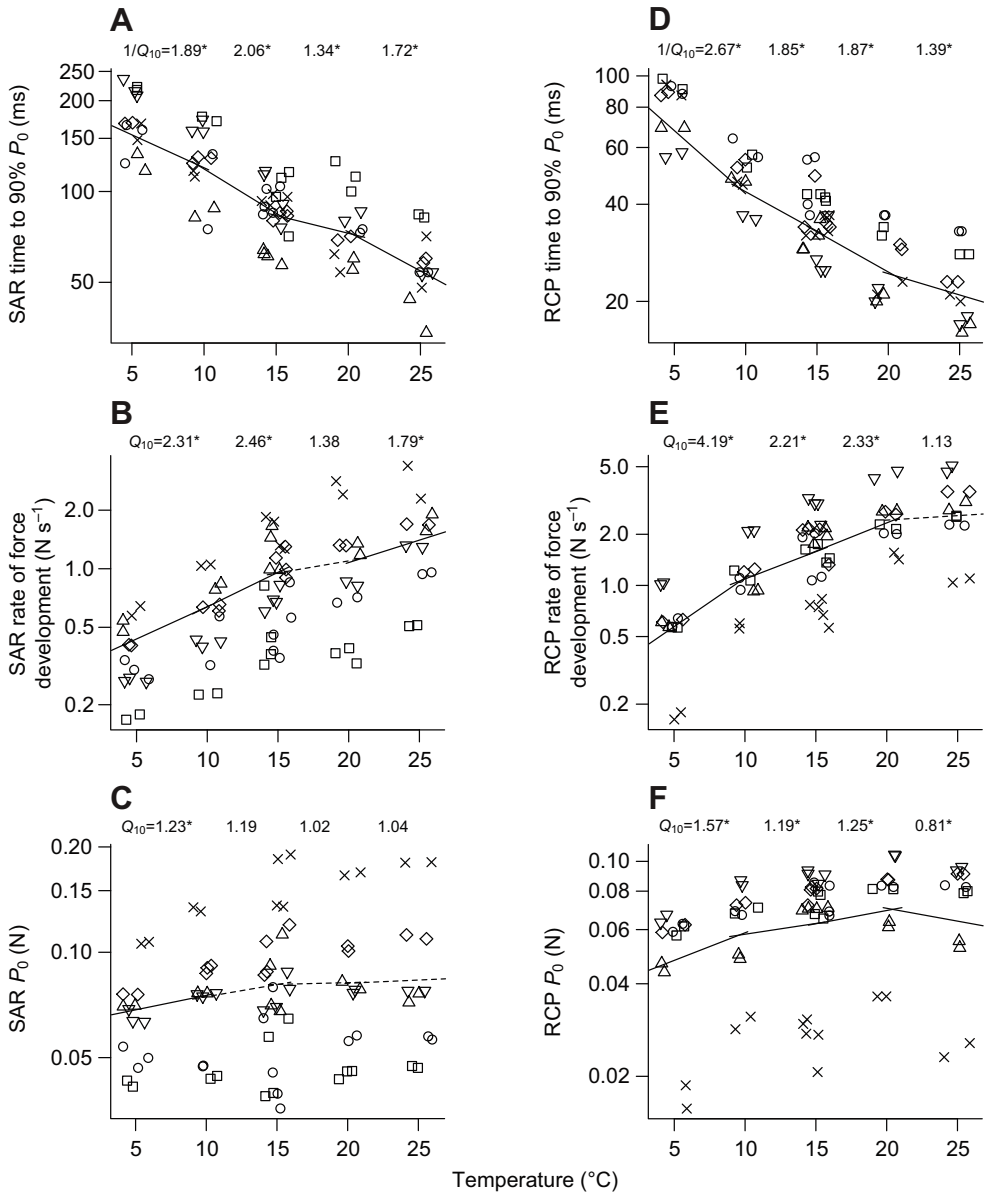

Fig. 6. Scatterplots of muscle contractile properties versus temperature. Note that data are from experiments conducted at 5, 10, 15, 20 and 25±1°C, yet data points are depicted here with random 'jitter' on the temperature axis to allow individual points to be discerned. A significant temperature effect for dynamic SAR variables (A–C) is depicted over each temperature interval, except for the rate of force development (B) across the 14–21°C interval, while a significant temperature effect for SAR peak isometric force (P_0) (C) is only depicted across the 4–11°C interval. A significant temperature effect for RCP variables (D–F), in contrast, is depicted over each temperature interval for each variable, except for the rate of force development (E) across the 14–21°C interval (see supplementary material Table S3 for details). Note that these data are from different individuals of *E. guttolineata* from the other figures. Indications as in Fig. 2.

projection, with an average activity duration of 91 ms. With tongue projection taking only 13 ms on average and tongue retraction on average taking only 50 ms, the RCP remained active throughout the tongue-retraction phase. The average duration of activity of the RCP prior to the onset of tongue retraction of only 14 ms is indicative of muscle-powered retraction without elastic storage prior to retraction.

The RCP may be limited in its ability to become active earlier as temperature declines, because doing so may interfere with tongue-projection performance. In fact, activity of the RCP was only significantly affected by temperature in its overall duration in the 4–11°C interval (supplementary material Table S2; Fig. 4, Fig. 5D–F). This lack of significance across the remaining temperature intervals corresponds to the lack of a significant thermal effect on tongue-projection duration in those intervals as well (supplementary material Table S2; Fig. 2B). This suggests that when tongue projection is thermally robust, the tongue-retractor muscle is not activated earlier relative to the onset of tongue projection. The tongue-retractor muscle in chameleons, which may also interfere with tongue-projection performance if activated early, displays a similar pattern, with a lack of temperature effects over a 15–35°C range (Anderson and Deban, 2012).

While intensity measures of EMG recordings for muscle associated with tongue projection in elastic systems studied previously have shown no effect of temperature (Deban and Lappin, 2011; Anderson and Deban, 2012), all intensity measures of the SAR in *E. guttolineata* in the 4–11°C interval are strongly reduced at lower temperatures (supplementary material Table S2; Fig. 4, Fig. 5C), coincident with declines in tongue-projection performance. These results indicate that *E. guttolineata* failed to recruit an equal number of muscle fibers below 11°C, and thus were likely unable to maximally load the tongue-projection mechanism at low temperature, resulting in reduced performance. Such declines in motor recruitment may be the result of decreased nerve conduction or altered motor unit recruitment patterns at low temperature (Rome, 1990). Importantly, the lack of an increase in intensity at low temperature indicates that, as hypothesized, the muscles were not recruited to a greater degree at different temperatures, for example, to compensate for a reduction of muscle contractile rate at lower temperatures.

Muscle contractile dynamics

In situ contractile experiments revealed that the SAR muscles, when stimulated isometrically, reached 90% P_0 in an average of 105 ms (Table 1, Fig. 6A). Given that the average latency between the onset of SAR activity and the onset of tongue projection was 123 ms (Table 1, Fig. 5B), this rate of force development should be sufficient for the SAR to fully load the projection mechanism with strain energy prior to the onset of tongue projection. This loading duration is similar to those seen before tongue projection in chameleons (146 ms) (Anderson and Deban, 2012) and toads (127 ms) (Deban and Lappin, 2011). As in *E. guttolineata*, the loading duration in chameleons is ample to fully load their projection mechanism, with the tongue-projector muscle reaching 90% P_0 in an average of 102 ms (Anderson and Deban, 2012).

The RCP muscles, when stimulated isometrically, reached 90% P_0 in an average of 42.5 ms (Table 1, Fig. 6D). Although the RCP became active on average 1.4 ms prior to the onset of tongue projection (Table 1, Fig. 5E), with an average tongue-projection duration of 13 ms (Table 1, Fig. 2B), the RCP is unlikely to have reached significant tension prior to the completion of tongue projection. In fact, based on the average activity onset time of the RCP and the average time to maximum projection distance at each experimental temperature, contractile data indicate that if the muscles were maximally activated *in vivo*, the RCP would reach an average tension of 1–31% P_0 by the time of maximal tongue projection, depending on temperature. Reaching its greatest level of tension during the tongue-retraction phase rather than prior to it would be beneficial because RCP activity would impinge less on tongue-projection performance.

As hypothesized, the dynamic contractile properties of the SAR and RCP were virtually all significantly affected by temperature across each temperature range (supplementary material Table S3; Fig. 6A,B,D,E). In both the SAR and RCP, however, Q_{10} and $1/Q_{10}$ values were higher for each variable in the lower two temperature intervals than in the higher two temperature intervals. This pattern is consistent with the pattern of significantly longer muscle activation times at the lower temperature interval, as well as a pattern of lower thermal dependence at higher temperatures for muscle contractile rates and rates of muscle-powered movements of other organisms (Bennett, 1984; Bennett, 1985; Putnam and Bennett, 1982; Hirano and Rome, 1984; John-Alder et al., 1989; Swoap et al., 1993; Stevenson and Josephson, 1990; Anderson and Deban, 2012).

P_0 of the SAR was significantly reduced by lower temperature only in the 4–11°C interval, while P_0 of the RCP was significantly affected by temperature over all temperature intervals (supplementary material Table S3; Fig. 6C,F). In all cases, however, Q_{10} values were considerably lower than those of dynamic variables from the same muscle across the same temperature interval, which is consistent with previously published data showing that static contractile properties exhibit lower thermal dependence than dynamic contractile properties (Bennett, 1985; Lutz and Rome, 1996; Anderson and Deban, 2012). The significant decline in peak tension as temperature decreases across the 4–11°C interval for the SAR contributes to a reduction in the total energy stored in elastic elements of the tongue that power tongue projection, and thus to the decline in tongue-projection performance across the same temperature interval (supplementary material Table S1; Fig. 2B,C, Fig. 3A–C).

Conclusions

Data presented here on the thermal dependence of elastic-recoil-powered tongue projection and muscle-powered tongue retraction in the plethodontid salamander *E. guttolineata* reveal that tongue-projection performance is maintained to a higher degree than tongue retraction performance across a wide temperature range. This thermal robustness is dependent on the tongue-projector muscles performing similar work at all temperatures and thus storing similar amounts of elastic energy in the elastic elements. Because muscle contractile rate declines with decreasing temperature, performing similar work is dependent on increased motor activity duration, equal burst intensity and similar tension development from the tongue-projector muscles as temperature declines. When one of these components fails to maintain function with declining temperature, whole-organism performance suffers despite the incorporation of an elastic-recoil mechanism.

The thermal robustness of independently evolved ballistic movements powered by elastic recoil is well established (see Anderson and Deban, 2010; Deban and Lappin, 2011; Deban and Richardson, 2011; Anderson and Deban, 2012; Sandusky and Deban, 2012). Clearly, there are considerable differences in ballistic tongue projection in frogs, toads, salamanders and chameleons in terms of the specific evolutionary modifications of their gross morphology, but despite these variations, they appear to have converged on similar patterns of interaction between morphological components and patterns of motor control, without apparent changes in muscle contractile physiology. Such modifications to morphology and motor patterns, specifically the elaboration of elastic tissues and the plasticity of muscle activation duration, appear to be sufficient to produce high performance and thermal robustness. At extreme temperatures, however, some species such as *E. guttolineata* still suffer from a loss of performance as motor control and muscle contraction ultimately succumb to thermal constraints. These species and conditions are informative about the limitations of the thermal robustness associated with these evolutionary adaptations, as they illustrate how high performance and functional robustness rely on the integrative nature of these elastically powered systems.

MATERIALS AND METHODS

Specimens

Eurycea guttolineata were collected in Macon and Jackson counties, NC, USA, and housed individually in plastic containers with a substrate of moist paper towels at 14–17°C at the University of South Florida. A total of 15 individuals (43–60 mm snout–vent length) that fed readily under observation were selected for kinematic and EMG recordings. An additional six individuals (55–68 mm snout–vent length) were used for muscle dynamics experiments. All procedures were approved by the Institutional Animal Care and Use Committee of the University of South Florida.

Electromyography

Bipolar patch electrodes were constructed from 50–75 cm strands of Formvar-coated, 0.025 mm diameter nichrome wire (A-M Systems no. 7615, Carlsborg, WA, USA) and 3×3 mm pieces of silicone that had been cut from 3.18 mm outer diameter, 1.98 mm inner diameter Silastic Laboratory Tubing (Dow Corning Corporation no. 508-009, Midland, MI, USA) in the form of an approximately one-third cylinder. Electrodes were made of two strands of wire threaded through the piece of tubing using a 27 gauge hypodermic needle. Strands were threaded through individually such that each strand entered through and exited out of the convex side of the tube, leaving two 1.5–2 mm sections of each wire running parallel to each other on the concave surface of the tube. Insulation from the wires on the concave surface was removed, and the ends of the wire were wrapped around the electrode lead. Electrodes were constructed in two configurations: one with the strands oriented parallel to the axis of the silicone cylinder, and the other with the strands oriented perpendicular to it.

Prior to electrode implantation, salamanders were anesthetized by immersion in a 1 g l^{-1} buffered aqueous solution of MS-222 (3-

aminobenzoic acid ethyl ester; Sigma, St Louis, MO, USA) for 10–30 min. Electrodes were implanted through two small incisions in the skin on the right side of the body, at the surface of the muscles. An electrode was placed against the SAR through an incision at the rostrocaudal level of the gular fold. A second electrode was placed against the RCP through an incision between the fifth and sixth costal groove. Electrodes were placed against the muscle surface with the concave surface cradling a portion of the cylindrical muscles and with the electrode configurations described above selected for each muscle such that the dipoles of the electrode lay parallel to the muscle fibers.

To accommodate large muscle movements and the delicate nature of the muscles, electrodes were not attached directly to the muscles. The electrodes were held in place by the concave shape of the silicone tubing and the overlying skin, allowing the muscle to move freely relative to the electrodes. Incisions were sutured closed. Electrode leads were glued together with modeling glue and attached to the skin of the salamander's back with a loop of suture to prevent them from becoming entangled or being pulled loose. The ends of the leads were stripped and soldered to a plug that mated with a socket on the amplifier probe.

EMG signals were amplified 1000–5000 times using a differential amplifier (A-M Systems 3500) and filtered to remove 60 Hz line noise. Signal output was mathematically adjusted *post hoc* to a common amplification level (1000 gain) to enable within-individual comparisons of signal amplitude. Conditioned signals were sampled at 4 kHz with a PowerLab 16/30 analog-to-digital converter coupled with LabChart software version 7 (ADInstruments, Bella Vista, NSW, Australia) running on an Apple MacBook Pro (Apple, Cupertino, CA, USA). EMG recordings were synchronized with digital images via a trigger shared with the camera.

Feeding experiments

After recovery from surgery (1–3 h), salamanders were imaged in dorsal view at 6 kHz frame rate and 1/12,000 s shutter speed with a Fastcam SA4 camera (Photron USA Inc., San Diego, CA, USA) as they fed on termites. All feeding trials and recordings were conducted within 5 days of surgery. Salamanders were placed on moistened grid paper on the surface of a temperature-controlled platform of a solid state heat/cool plate (ThermoElectric Cooling America Corporation no. AHP-1200CPV, Chicago, IL, USA) and covered with a moistened paper towel to provide a retreat. Immediately prior to filming, the moistened paper towel covering the salamander was folded back to expose just the head and a termite was dropped in front of the salamander at varying distances.

Feeding trials were conducted across a range of experimental temperatures (5–25°C) at 5°C increments by adjusting the temperature of the platform. The temperature sequence of feeding trials for each individual was in random order with one to three feedings per experimental temperature, depending on the willingness of the salamander to feed, before attempting a new temperature. Salamanders were allowed to acclimate at the experimental temperature for a period of at least 20 min prior to feeding trials. To prevent elevation of body temperature through light-source radiation, a 36×1 W white (5500 K) LED light panel (LED Wholesalers no. 2510W, Hayward, CA, USA) was used for supplemental lighting. As the salamander was pressed against a moistened surface on top of the temperature platform, its body temperature closely matched the temperature of the platform. Body temperature was verified on the dorsal surface of the head using a calibrated infrared thermometer (±1°C accuracy; Sixth Sense LT300, Williston, VT, USA) at close range following every feeding event. Salamander temperatures ranged from 4.9 to 25.1°C.

Muscle contraction experiments

For all muscle contraction experiments, muscles were attached to a dual servo-motor force lever (Aurora Scientific, Inc., Model 305C-LR, Aurora, ON, Canada) by Spiderwire microfilament (Pure Fishing, Inc., Spirit Lake, IA, USA), for which previous viscoelastic property examination found no observable oscillations during rapid force reduction (Lappin et al., 2006). During stimulation experiments, the muscle preparation was located in the inner chamber of a tissue–organ bath (Model 805A, Aurora Scientific) filled with oxygenated amphibian Ringer's solution. The tissue–organ bath was maintained at a set temperature with a temperature-controlled water circulator (IsoTemp 1013S, Fisher Scientific, Waltham, MA, USA) and bath temperature was monitored with a thermometer in the bath. Force and position from the lever and stimulation pulses from the stimulator (Model 701B, Aurora Scientific) were recorded with an analog-to-digital interface (Model 604A, Aurora Scientific) connected to an Apple PowerMac G4 computer running a custom-made LabVIEW 8.2 virtual instrument with a PCI-6221 data acquisition card (National Instruments, Austin, TX, USA) sampling at 1000 Hz.

Prior to muscle excision for contractile experiments, salamanders were killed by double-pithing. The salamander's tongue was extended out of the mouth to maximum tongue-projection distance. The distance from the RCP origin at the pelvis to the lower jaw tip, the distance from the lower jaw tip to the basibranchial tip at maximum tongue projection and the distance from the distal tip of the epibranchial to the basibranchial tip at maximum tongue projection were each measured using digital calipers (±0.1 mm accuracy; Mitutoyo 700-126, Kawasaki-shi, Kanagawa, Japan) so that the length of an excised portion of the RCP could be matched to its length at maximum tongue projection. The RCP muscles were severed at the epibranchial tips with the tongue fully extended, then severed at their origins on the pelvis and gently withdrawn from the body at the pelvis. The excised portions of the RCP were wrapped in a paper towel moistened with amphibian Ringer's solution and allowed to rest at 5°C for use immediately following contractile data collection from the SAR of the same salamander.

Contractile experiments for the SAR were collected using an *in situ* preparation. The skin was removed from the ventral side of the salamander's head and Spiderwire was tied around the basibranchial at the articulation with the first ceratobranchial pair. A second strand of Spiderwire was then tied around the lower jaw at the mandibular symphysis and a third strand was wrapped around the head to keep the upper and lower jaws closed and the tongue skeleton from rotating ventrally. Bipolar patch electrodes were constructed and implanted bilaterally on the surface of the SAR in a similar fashion to the SAR EMG electrodes described above. The salamander was then tied to an assembly that was suspended within the oxygenated Ringer's bath. A Spiderwire strand attached to the lower jaw was anchored to the bottom of the assembly and the Spiderwire strand attached to the basibranchial was extended posteriorly adjacent and parallel to the ventral surface of the body to the force lever mounted above at the salamander's caudal end. The position of the stimulation chamber was then adjusted until all slack in the Spiderwire between the base of the stimulation chamber and the muscle lever was removed. This setup thus allowed for the force produced by the SAR muscles acting to push the epibranchials out of the mouth to be measured at the basibranchial.

Contractile experiments for the RCP were collected using a standard *in vitro* preparation. The excised RCP sample was removed from 5°C storage for experimentation no longer than 2.5 h following excision. The paired muscle sample was tied off with Spiderwire such that when the entire sample was extended to its length at maximal tongue projection, the tied off portion was 2.0–3.0 cm long. The Spiderwire on one end of the sample was anchored to the bottom of the electrode assembly within the stimulation chamber and the Spiderwire on the other end was attached to the end of the force lever so that the muscle was located between the platinum-coated electrodes of a bi-polar pulse stimulator. The position of the electrode assembly was then adjusted until the sample was extended to its length at maximum tongue projection.

Isometric contractions from each muscle were elicited with 80 V supramaximal stimulations at a frequency of 160 pulses s^{-1} and a current of 500 mA to achieve fused tetanus. The muscles were stimulated two to three times at each temperature in the assigned temperature sequence. A 10 min rest period between stimulations at the same temperature and a 20 min acclimation period to each experimental temperature were allowed. In order to adjust for muscle fatigue over the period of muscle contractions, each muscle was subjected to an experimental temperature sequence that began and ended at 15°C and the muscles were divided equally between two temperature sequences: 15–5–10–20–25–15°C and 15–25–20–10–5–15°C. This eliminated any tendency of muscle fatigue to produce trends across a range of temperatures by allowing the initial and final sets of contractions at a given temperature to be averaged, and by ensuring that no one temperature was sampled on average earlier or later in the sequence than another.

Kinematic and dynamic analyses

The digital image sequences were used to quantify the timing and amplitude of movements of the tongue during prey capture, with respect to the upper jaw tip as a fixed reference. The *x*, *y* coordinates of the tongue tip and the tip of the upper jaw were recorded from the image sequences using ImageJ software (National Institutes of Health, Bethesda, MD, USA) running on an Apple iMac computer. Coordinates were recorded starting with the first appearance of the tongue beyond the upper jaw during tongue projection and ending with the withdrawal of the tongue pad into the mouth at the end of tongue retraction. Tongue-projection distance was computed as the greatest distance between these position data points. A 5 mm grid under the salamander calibrated the distances for each feeding. Additionally, two events were identified in the image sequences and their times measured relative to the start of ballistic tongue projection at time zero: (1) maximum tongue projection, the time at which the leading edge of the tongue pad was the greatest distance from the tip of the upper jaw, and (2) the end of tongue retraction, the time at which the tongue pad fully withdrew into the mouth following tongue projection. Average velocities of tongue projection and tongue retraction were calculated from these measurements.

The dynamics of tongue movements were calculated by fitting a quintic spline to the distance data with the Pspline package in R statistical software (www.r-project.org). First and second derivatives of the spline function were computed to produce instantaneous velocity and acceleration, respectively, at an interpolated rate of 10 kHz. The smoothing parameter of the spline was adjusted to remove secondary oscillation artifacts from the first and second derivatives of the fitted trace. Instantaneous mass-specific power was calculated as the product of velocity at a given point in time and the corresponding acceleration. The maximum kinetic energy during tongue projection was then calculated as the product of half of the squared peak projection velocity and the average mass of the tongue projectile, as measured from the dissection of the six *E. guttolineata* specimens from the muscle contractile experiments. Muscle mass-specific maximum kinetic energy and power during tongue projection was calculated by multiplying the maxima of these parameters by the average ratio of the mass of the tongue projectile to the mass of the SAR muscles for the specimens used in contractile experiments (1.14±0.47, mean ± s.e.m.). Finally, muscle mass-specific power during tongue retraction was calculated by multiplying the maxima by the average ratio of the mass of the tongue projectile to the mass of the RCP muscles for the specimens used in contractile experiments (1.20±0.49).

Analysis of electromyograms

The amplitudes of activity of the SAR and RCP and their timing of activity relative to kinematic events were quantified from the rectified EMG signals using AD Instruments LabChart software running on an Apple MacBook Pro. For both the SAR and RCP, activity durations, as well as latencies from the onset of activity and peak activity (peak of r.m.s.) to associated kinematic events were measured. Onset of activity was defined as the time after which the EMG amplitude reached twice the background noise level for at least 10 ms and the end of activity was similarly defined as the signal dropping below twice the noise level after which it remained there for at least 10 ms. Six latency durations were measured: (1) SAR activity onset to the start of tongue projection, (2) peak of SAR activity to the start of tongue projection, (3) SAR activity offset to the start of tongue projection, (4) RCP activity onset to the start of tongue projection, (5) RCP activity onset to the time of maximal tongue projection and (6) peak of RCP activity to the time of maximal tongue projection.

Amplitude and intensity variables were measured between the onset and end of activity of each muscle. Integrated area was measured as the sum of the values of the rectified signal over the activity time periods. Intensity of the EMG bursts was measured as (1) the r.m.s. of the values of the signal within the activity time periods and (2) the integrated area divided by the duration of those activity time periods. The peak amplitude of muscle activity was measured as the maximum r.m.s. value using a 20 ms time constant (i.e. the moving 20 ms time window over which the r.m.s. was calculated).

Analysis of muscle contractile data

Electromechanical delay, and static and dynamic contractile characteristics of isometric contractions of both the SAR and RCP were quantified from raw stimulation, force and length outputs using Microsoft Excel 2004 for Mac OS X running on an Apple MacBook Pro. P_0 was quantified as the maximum force recorded from each trace and 90% P_0 was calculated based on that value. The time of the start of stimulation was quantified as the first spike in voltage from the recorded stimulation trace. The time of the start of force production was quantified as the first time following the onset of stimulation after which force over the following 6 ms increased consecutively. Subsequent timing events were measured relative to the start of force production at time zero. The time to 90% P_0 was quantified as the time when the force trace first equaled or surpassed the calculated 90% P_0 value. The electromechanical delay was calculated as the latency between the onset of stimulation and the start of force production. The time to 90% P_0 was calculated as the latency between the start of force production and the time of 90% P_0. The rate of force development was then calculated as the 90% P_0 value divided by the time to 90% P_0.

Statistical analyses

All performance, EMG and contractile data were $\log_{10}$ transformed prior to statistical analysis because these variables were expected to have an exponential relationship with temperature. All data were divided into four overlapping intervals (4–11, 9–16, 14–21 and 19–26°C) based on the temperature at which the data were gathered to examine whether the thermal relationship varied across the temperature range. An ANCOVA was conducted separately on each subset of the data on an Apple iMac computer using JMP 5.1 software (SAS Institute, Cary, NC, USA). Significance levels were adjusted to control for false discovery rate in multiple comparisons (Benjamini and Hochberg, 1995).

Prior to $\log_{10}$ transformation and statistical analysis, EMG timing variables were examined for negative values. Some kinematic events were variable with regard to whether they began before or after muscle activity onset; therefore, some timing variables included negative time data. Any variable that included negative data points was offset by one unit over its lowest value to allow for proper $\log_{10}$ transformation.

Performance and EMG data were then tested for three effects: (1) temperature, (2) individual and (3) projection distance. Muscle contraction data were tested for two effects on the variables: (1) temperature and (2) individual. In both models, a random individual effect was included to account for body size and other random individual differences. Temperature effects were included as a continuous variable to examine how elastically powered and non-elastic movements responded to changes in body temperature. Projection distance was included in the performance and EMG model to account for potential effects on those variables, but in order to increase sample size and statistical power, it was dropped from the model when non-significant for a given variable.

Temperature coefficients (Q_{10}) were computed across each temperature interval (4–11, 9–16, 14–21 and 19–26°C) for each variable as the base 10 anti-logarithm of the partial regression coefficients (PRCs) of the temperature effect in the ANCOVA multiplied by 10 (Deban and Lappin, 2011; Deban and Richardson, 2011; Anderson and Deban, 2012; Sandusky and Deban, 2012). The ANCOVA models include effects of individual (and projection distance for relevant performance and EMG data) that influence the estimate of the relationship between the variable and temperature, so calculation of Q_{10} values from the PRC accounts for these effects as well. To express duration variables as rates, the temperature coefficients for these variables were reported as inverse Q_{10} values (i.e. $1/Q_{10}$).

Acknowledgements

We thank Jared Caban, Shelby Creemers, Arturo Fernandez, Lauren Grant, Segall Israel and Paula Sandusky for data collection and analysis assistance, and Jeffrey Olberding, Charlotte Stinson and two anonymous reviewers for helpful comments on earlier versions of the manuscript.

Competing interests

The authors declare no competing financial interests.

Author contributions

C.V.A. and S.M.D. designed the study. All authors were involved in data collection. C.V.A. and S.M.D. analyzed the data and all authors played a role in writing the manuscript.

Funding
This research was supported by National Science Foundation grants IOS 0842626 and IOS 1350929 to S.M.D. and by the University of South Florida System Research & Innovation Internal Awards Program under grant no. 0057245 to S.M.D.

Supplementary material
Supplementary material available online at
http://jeb.biologists.org/lookup/suppl/doi:10.1242/jeb.105437/-/DC1

References
Alexander, R. M. (1966). Rubber-like properties of the inner hinge-ligament of Pectinidae. *J. Exp. Biol.* **44**, 119-130.
Anderson, C. V. and Deban, S. M. (2010). Ballistic tongue projection in chameleons maintains high performance at low temperature. *Proc. Natl. Acad. Sci. USA* **107**, 5495-5499.
Anderson, C. V. and Deban, S. M. (2012). Thermal effects on motor control and *in vitro* muscle dynamics of the ballistic tongue apparatus in chameleons. *J. Exp. Biol.* **215**, 4345-4357.
Anderson, C. V. and Higham, T. E. (2014). Chameleon anatomy. In *The Biology of Chameleons* (ed. K. A. Tolley and A. Herrel), pp. 7-55. Berkeley, CA: University of California Press.
Astley, H. C. and Roberts, T. J. (2012). Evidence for a vertebrate catapult: elastic energy storage in the plantaris tendon during frog jumping. *Biol. Lett.* **8**, 386-389.
Benjamini, Y. and Hochberg, Y. (1995). Controlling the false discovery rate: a practical and powerful approach to multiple testing. *J. R. Stat. Soc. B* **57**, 289-300.
Bennett, A. F. (1984). Thermal dependence of muscle function. *Am. J. Physiol.* **247**, R217-R229.
Bennett, A. F. (1985). Temperature and muscle. *J. Exp. Biol.* **115**, 333-344.
Burrows, M. (2006). Jumping performance of froghopper insects. *J. Exp. Biol.* **209**, 4607-4621.
Burrows, M. (2009). How fleas jump. *J. Exp. Biol.* **212**, 2881-2883.
de Groot, J. H. and van Leeuwen, J. L. (2004). Evidence for an elastic projection mechanism in the chameleon tongue. *Proc. R. Soc. B* **271**, 761-770.
Deban, S. M. and Dicke, U. (1999). Motor control of tongue movement during prey capture in plethodontid salamanders. *J. Exp. Biol.* **202**, 3699-3714.
Deban, S. M. and Dicke, U. (2004). Activation patterns of the tongue-projector muscle during feeding in the imperial cave salamander *Hydromantes imperialis*. *J. Exp. Biol.* **207**, 2071-2081.
Deban, S. M. and Lappin, A. K. (2011). Thermal effects on the dynamics and motor control of ballistic prey capture in toads: maintaining high performance at low temperature. *J. Exp. Biol.* **214**, 1333-1346.
Deban, S. M. and Richardson, J. C. (2011). Cold-blooded snipers: thermal independence of ballistic tongue projection in the salamander *Hydromantes platycephalus*. *J. Exp. Zool.A* **315**, 618-630.
Deban, S. M., Wake, D. B. and Roth, G. (1997). Salamander with a ballistic tongue. *Nature* **389**, 27.
Deban, S. M., O'Reilly, J. C., Dicke, U. and van Leeuwen, J. L. (2007). Extremely high-power tongue projection in plethodontid salamanders. *J. Exp. Biol.* **210**, 655-667.
Denny, M. and Miller, L. (2006). Jet propulsion in the cold: mechanics of swimming in the Antarctic scallop *Adamussium colbecki*. *J. Exp. Biol.* **209**, 4503-4514.
Herrel, A., James, R. S. and Van Damme, R. (2007). Fight versus flight: physiological basis for temperature-dependent behavioral shifts in lizards. *J. Exp. Biol.* **210**, 1762-1767.
Higham, T. E. and Anderson, C. V. (2014). Function and adaptation of chameleons. In *The Biology of Chameleons* (ed. K. A. Tolley and A. Herrel), pp. 63-83. Berkeley, CA: University of California Press.
Hirano, M. and Rome, L. C. (1984). Jumping performance of frogs (*Rana pipiens*) as a function of muscle temperature. *J. Exp. Biol.* **108**, 429-439.
Huey, R. B. and Stevenson, R. D. (1979). Integrative thermal physiology and ecology of ectotherms: a discussion of approaches. *Am. Zool.* **19**, 357-366.
James, R. S. (2013). A review of the thermal sensitivity of the mechanics of vertebrate skeletal muscle. *J. Comp. Physiol. B* **183**, 723-733.
John-Alder, H. B., Barnhart, M. C. and Bennett, A. F. (1989). Thermal sensitivity of swimming performance and muscle contraction in northern and southern populations of tree frogs (*Hyla crucifer*). *J. Exp. Biol.* **142**, 357-372.
Lappin, A. K., Monroy, J. A., Pilarski, J. Q., Zepnewski, E. D., Pierotti, D. J. and Nishikawa, K. C. (2006). Storage and recovery of elastic potential energy powers ballistic prey capture in toads. *J. Exp. Biol.* **209**, 2535-2553.
Lombard, R. E. and Wake, D. B. (1976). Tongue evolution in the lungless salamanders, family Plethodontidae. I. Introduction, theory and a general model of dynamics. *J. Morphol.* **148**, 265-286.
Lutz, G. J. and Rome, L. C. (1994). Built for jumping: the design of the frog muscular system. *Science* **263**, 370-372.
Lutz, G. J. and Rome, L. C. (1996). Muscle function during jumping in frogs. II. Mechanical properties of muscle: implications for system design. *Am. J. Physiol.* **271**, C571-C578.
Nishikawa, K. C. (2000). Feeding in frogs. In *Feeding: Form, Function, and Evolution in Tetrapod Vertebrates* (ed. K. Schwenk), pp. 117-147. San Diego, CA: Academic Press.
Patek, S. N., Korff, W. L. and Caldwell, R. L. (2004). Biomechanics: deadly strike mechanism of a mantis shrimp. *Nature* **428**, 819-820.
Patek, S. N., Baio, J. E., Fisher, B. L. and Suarez, A. V. (2006). Multifunctionality and mechanical origins: ballistic jaw propulsion in trap-jaw ants. *Proc. Natl. Acad. Sci. USA* **103**, 12787-12792.
Patek, S. N., Nowroozi, B. N., Baio, J. E., Caldwell, R. L. and Summers, A. P. (2007). Linkage mechanics and power amplification of the mantis shrimp's strike. *J. Exp. Biol.* **210**, 3677-3688.
Putnam, R. W. and Bennett, A. F. (1982). Thermal dependence of isometric contractile properties of lizard muscle. *J. Comp. Physiol. B* **147**, 11-20.
Rigby, B. J., Hirai, N., Spikes, J. D. and Eyring, H. (1959). The mechanical properties of rat tail tendon. *J. Gen. Physiol.* **43**, 265-283.
Roberts, T. J. and Azizi, E. (2011). Flexible mechanisms: the diverse roles of biological springs in vertebrate movement. *J. Exp. Biol.* **214**, 353-361.
Roberts, T. J. and Marsh, R. L. (2003). Probing the limits to muscle-powered accelerations: lessons from jumping bullfrogs. *J. Exp. Biol.* **206**, 2567-2580.
Rome, L. C. (1990). Influence of temperature on muscle recruitment and muscle function *in vivo*. *Am. J. Physiol.* **259**, R210-R222.
Sandusky, P. E. and Deban, S. M. (2012). Temperature effects on the biomechanics of prey capture in the frog *Rana pipiens*. *J. Exp. Zool. A.* **317**, 595-607.
Stevenson, R. D. and Josephson, R. K. (1990). Effects of operating frequency and temperature on mechanical power output from moth flight muscle. *J. Exp. Biol.* **149**, 61-78.
Swoap, S. J., Johnson, T. P., Josephson, R. K. and Bennett, A. F. (1993). Temperature, muscle power output and limitations on burst locomotor performance of the lizard *Dipsosaurus dorsalis*. *J. Exp. Biol.* **174**, 185-197.
Van Wassenbergh, S., Strother, J. A., Flammang, B. E., Ferry-Graham, L. A. and Aerts, P. (2008). Extremely fast prey capture in pipefish is powered by elastic recoil. *J. R. Soc. Interface* **5**, 285-296.
Vieites, D. R., Román, S. N., Wake, M. H. and Wake, D. B. (2011). A multigenic perspective on phylogenetic relationships in the largest family of salamanders, the Plethodontidae. *Mol. Phylogenet. Evol.* **59**, 623-635.
Vogel, S. (2003). *Comparative Biomechanics: Life's Physical World*, pp. 582. Princeton, NJ: Princeton University Press.
Wake, D. B. and Deban, S. M. (2000). Terrestrial feeding in salamanders. In *Feeding* (ed. K. Schwenk), pp. 95-116. San Diego, CA: Academic Press.
Wainwright, P. C. and Bennett, A. F. (1992a). The mechanism of tongue projection in chameleons. I. Electromyographic tests of functional hypotheses. *J. Exp. Biol.* **168**, 1-21.
Wainwright, P. C. and Bennett, A. F. (1992b). The mechanism of tongue projection in chameleons. II. Role of shape change in a muscular hydrostat. *J. Exp. Biol.* **168**, 23-40.

Table S1. Results of ANCOVA examining effects on kinematic and dynamic variables in *Eurycea guttolineata* over four temperature intervals.

	Individual	Temperature	Projection Distance	Temperature		
	P-value	*P*-value	*P*-value	Slope	Q_{10}	1/ Q_{10}
4-11ºC						
Projection distance	0.6009	0.2150	-	0.0113	1.30	0.77
Duration of tongue projection	**0.0005**	**<0.0001**	0.1234	-0.0774	0.17	**5.95**
Duration of tongue retraction	**0.0004**	**0.0004**	0.0655	-0.0307	0.49	**2.03**
Peak projection velocity	**<0.0001**	**0.0001**	**<0.0001**	0.0306	**2.03**	0.49
Average projection velocity	**0.0006**	**<0.0001**	**<0.0001**	0.0709	**5.12**	0.20
Peak projection acceleration	**0.0002**	**<0.0001**	**0.0334**	0.0701	**5.03**	0.20
Peak projection specific power	**<0.0001**	**<0.0001**	**0.0004**	0.0973	**9.39**	0.11
Peak retraction velocity	**0.0003**	**0.0009**	0.0524	0.0356	**2.27**	0.44
Average retraction velocity	**0.0013**	**0.0005**	**<0.0001**	0.0329	**2.13**	0.47
Peak retraction acceleration	**0.0071**	**0.0007**	0.9322	0.0558	**3.61**	0.28
Peak retraction specific power	**0.0010**	**0.0006**	0.7267	0.0903	**7.99**	0.13
9-16ºC						
Projection distance	0.4725	0.7385	-	-0.0030	0.93	1.07
Duration of tongue projection	**<0.0001**	0.3707	0.1126	-0.0095	0.80	1.24
Duration of tongue retraction	**0.0228**	0.0532	0.2672	-0.0265	0.54	1.84
Peak projection velocity	**<0.0001**	0.2413	**<0.0001**	0.0050	1.12	0.89
Average projection velocity	**<0.0001**	0.5313	**<0.0001**	0.0066	1.16	0.86
Peak projection acceleration	**<0.0001**	0.0696	**0.0077**	0.0206	1.61	0.62
Peak projection specific power	**<0.0001**	0.0427	**<0.0001**	0.0288	1.94	0.52
Peak retraction velocity	**0.0003**	**0.0003**	0.0508	0.0341	**2.19**	0.46
Average retraction velocity	**0.0310**	0.0765	**0.0010**	0.0236	1.72	0.58
Peak retraction acceleration	**0.0303**	**0.0004**	0.2933	0.0632	**4.28**	0.23
Peak retraction specific power	**0.0069**	**0.0001**	0.7583	0.0987	**9.70**	0.10
14-21ºC						
Projection distance	**0.0043**	0.3677	-	0.0070	1.18	0.85
Duration of tongue projection	**<0.0001**	0.1378	0.4132	-0.0116	0.77	1.31
Duration of tongue retraction	**0.0028**	**0.0008**	0.6298	-0.0366	0.43	**2.32**
Peak projection velocity	**<0.0001**	0.5072	**<0.0001**	-0.0029	0.94	1.07
Average projection velocity	**<0.0001**	0.3346	**<0.0001**	0.0082	1.21	0.83
Peak projection acceleration	**<0.0001**	0.9565	**0.0026**	-0.0005	0.99	1.01
Peak projection specific power	**<0.0001**	0.6114	**<0.0001**	-0.0063	0.86	1.16
Peak retraction velocity	**0.0111**	0.0342	**0.0194**	0.0160	1.44	0.69
Average retraction velocity	**0.0029**	**0.0014**	**<0.0001**	0.0350	**2.24**	0.45
Peak retraction acceleration	**0.0001**	0.0896	0.1736	0.0245	1.76	0.57
Peak retraction specific power	**0.0002**	0.0265	0.6758	0.0439	2.74	0.36
19-26ºC						
Projection distance	**0.0012**	0.1323	-	0.0104	1.27	0.79
Duration of tongue projection	**<0.0001**	0.0451	0.3683	-0.0128	0.74	1.34
Duration of tongue retraction	**0.0003**	**0.0071**	0.7584	-0.0169	0.68	**1.48**
Peak projection velocity	**<0.0001**	0.3794	**<0.0001**	0.0034	1.08	0.93
Average projection velocity	**<0.0001**	0.0507	**<0.0001**	0.0147	1.40	0.71
Peak projection acceleration	**<0.0001**	0.7431	**0.0269**	0.0029	1.07	0.93
Peak projection specific power	**<0.0001**	0.6773	**<0.0001**	0.0046	1.11	0.90
Peak retraction velocity	**0.0015**	**0.0004**	**0.0009**	0.0220	**1.66**	0.60
Average retraction velocity	**0.0001**	**0.0082**	**<0.0001**	0.0180	**1.52**	0.66
Peak retraction acceleration	**<0.0001**	0.1877	0.7637	0.0208	1.61	0.62
Peak retraction specific power	**0.0002**	0.0256	0.5341	0.0438	2.74	0.37

P-values are shown for individual and temperature, as in the partial regression coefficient for the temperature effect (i.e., slope) from the model from which Q_{10} values were calculated. Projection distance was included as a covariate only when it showed a significant effect for that variable.

Bold *P*-values indicate significance levels adjusted to correct for false discovery rate (Benjamini and Hockberg, 1995). Bold Q_{10} values indicate significant temperature effects.

Table S2. Results of ANCOVA examining effects on electromyographic amplitude and duration variables in *Eurycea guttolineata* over four temperature intervals.

	Individual	Temperature	Projection Distance	Temperature		
	P-value	*P*-value	*P*-value	Slope	Q_{10}	1/ Q_{10}
4-11ºC						
SAR activity duration	0.0286	**0.0008**	**0.0034**	-0.0308	0.49	**2.03**
SAR onset to tongue projection onset duration	0.1194	**<0.0001**	**0.0001**	-0.0320	0.48	**2.09**
SAR max. amplitude to tongue projection duration	0.3901	0.8850	0.2276	-0.0026	0.94	1.06
SAR offset to tongue projection onset duration	0.6108	0.9835	0.1186	0.0005	1.01	0.99
SAR r.m.s.	**0.0001**	**0.0003**	0.8934	0.0623	**4.19**	0.24
SAR integrated area/duration	**<0.0001**	**0.0018**	0.5942	0.0600	**3.98**	0.25
SAR r.m.s. max. amplitude	**0.0001**	**0.0010**	0.8688	0.0575	**3.76**	0.27
RCP activity duration	0.2693	**0.0002**	0.8732	-0.0477	0.33	**3.00**
RCP onset to tongue projection duration	0.0871	0.5868	0.2006	0.0039	1.09	0.91
RCP onset to max. tongue projection duration	0.0427	0.2243	0.4740	-0.0102	0.79	1.27
RCP max. amplitude to max. projection duration	**0.0155**	0.3382	0.4401	0.0007	1.02	0.98
RCP r.m.s.	**<0.0001**	0.4900	0.7104	0.0229	1.70	0.59
RCP integrated area/duration	**<0.0001**	0.5419	0.7050	0.0200	1.58	0.63
RCP r.m.s. max. amplitude	**<0.0001**	0.9325	0.7176	0.0029	1.07	0.94
9-16ºC						
SAR activity duration	**0.0011**	**0.0001**	0.7113	-0.0267	0.54	**1.85**
SAR onset to tongue projection onset duration	0.1279	**<0.0001**	0.0040	-0.0291	0.51	**1.96**
SAR max. amplitude to tongue projection duration	0.1178	**0.0008**	0.3101	-0.0494	0.32	**3.12**
SAR offset to tongue projection onset duration	0.3279	0.6260	0.1688	-0.0197	0.64	1.57
SAR r.m.s.	**<0.0001**	0.0232	0.1925	0.0183	1.52	0.66
SAR integrated area/duration	**<0.0001**	0.3594	0.1206	0.0098	1.25	0.80
SAR r.m.s. max. amplitude	**<0.0001**	0.4411	0.3935	0.0067	1.17	0.86
RCP activity duration	0.2479	0.2205	0.7657	-0.0121	0.76	1.32
RCP onset to tongue projection duration	0.3481	0.9614	0.1352	-0.0012	0.97	1.03
RCP onset to max. tongue projection duration	0.3633	0.9663	0.1727	-0.0017	0.96	1.04
RCP max. amplitude to max. projection duration	0.1710	0.3693	0.0376	-0.0006	0.99	1.01
RCP r.m.s.	**<0.0001**	0.2191	0.4802	0.0251	1.78	0.56
RCP integrated area/duration	**<0.0001**	0.2441	0.4811	0.0237	1.73	0.58
RCP r.m.s. max. amplitude	**<0.0001**	0.2941	0.3686	0.0216	1.65	0.61
14-21ºC						
SAR activity duration	**0.0047**	0.0440	0.8340	-0.0114	0.77	1.30
SAR onset to tongue projection onset duration	0.0560	**<0.0001**	**0.0027**	-0.0178	0.66	**1.51**

SAR max. amplitude to tongue projection duration	**0.0001**	0.7847	0.2930	-0.0046	0.90	1.11
SAR offset to tongue projection onset duration	0.1815	0.6556	0.0781	0.0135	1.37	0.73
SAR r.m.s.	**<0.0001**	**0.0092**	0.2994	0.0171	**1.48**	0.67
SAR integrated area/duration	**<0.0001**	0.0535	0.2026	0.0132	1.35	0.74
SAR r.m.s. max. amplitude	**<0.0001**	**0.0063**	0.3850	0.0190	**1.55**	0.65
RCP activity duration	0.3058	0.6304	0.3753	-0.0043	0.91	1.10
RCP onset to tongue projection duration	0.7448	0.2245	0.4757	0.0241	1.74	0.57
RCP onset to max. tongue projection duration	0.8140	0.2499	0.5011	0.0372	2.36	0.42
RCP max. amplitude to max. projection duration	0.9847	0.4282	0.6432	-0.0321	0.48	2.09
RCP r.m.s.	**<0.0001**	0.1997	0.4523	-0.0205	0.62	1.60
RCP integrated area/duration	**<0.0001**	0.3412	0.4021	-0.0155	0.70	1.43
RCP r.m.s. max. amplitude	**<0.0001**	0.1093	0.2731	-0.0256	0.55	1.80
19-26ºC						
SAR activity duration	**0.0115**	0.0214	0.9000	-0.0127	0.75	1.34
SAR onset to tongue projection onset duration	0.2365	**<0.0001**	0.0152	-0.0201	0.63	**1. 59**
SAR max. amplitude to tongue projection duration	0.2654	0.6515	0.5865	0.0092	1.24	0.81
SAR offset to tongue projection onset duration	0.0599	0.5201	0.0654	-0.0032	0.93	1.08
SAR r.m.s.	**<0.0001**	0.5986	0.8557	0.0034	1.08	0.92
SAR integrated area/duration	**<0.0001**	0.8546	0.9414	0.0013	1.03	0.97
SAR r.m.s. max. amplitude	**<0.0001**	0.4472	0.7627	0.0050	1.12	0.89
RCP activity duration	0.0500	0.1209	0.2159	-0.0115	0.77	1.30
RCP onset to tongue projection duration	**0.0078**	0.8375	0.7536	-0.0006	0.99	1.01
RCP onset to max. tongue projection duration	**0.0034**	0.5953	0.7566	-0.0019	0.96	1.05
RCP max. amplitude to max. projection duration	0.9875	0.3648	0.4255	0.0401	2.52	0.40
RCP r.m.s.	**<0.0001**	0.5782	0.6183	-0.0117	0.76	1.31
RCP integrated area/duration	**<0.0001**	0.2314	0.6735	-0.0254	0.56	1.79
RCP r.m.s. max. amplitude	**<0.0001**	0.4867	0.7273	-0.0144	0.72	1.39

P-values are shown for individual and temperature, as in the partial regression coefficient for the temperature effect (i.e., slope) from the model from which Q_{10} values were calculated. Projection distance was included as a covariate only when it showed a significant effect for that variable.

Bold *P*-values indicate significance levels adjusted to correct for false discovery rate (Benjamini and Hockberg, 1995). Bold Q_{10} values indicate significant temperature effects.

Table S3. Results of ANCOVA examining effects on contractile variables in *Eurycea guttolineata* over four temperature intervals.

	Individual	Temperature	Temperature		
	P-value	*P*-value	Slope	Q_{10}	1/ Q_{10}
4-11ºC					
SAR peak isometric force (P_0)	**<0.0001**	**0.0002**	0.0089	**1.23**	0.82
SAR time to 90% P_0	**<0.0001**	**<0.0001**	-0.0276	0.53	**1.89**
SAR rate of force development	**<0.0001**	**<0.0001**	0.0365	**2.31**	0.43
SAR electromechanical delay	**<0.0001**	**<0.0001**	-0.0388	0.41	**2.44**
RCP peak isometric force (P_0)	**<0.0001**	**<0.0001**	0.0196	**1.57**	0.64
RCP time to 90% P_0	**<0.0001**	**<0.0001**	-0.0426	0.37	**2.67**
RCP rate of force development	**<0.0001**	**<0.0001**	0.0622	**4.19**	0.24
RCP electromechanical delay	**<0.0001**	**<0.0001**	-0.0441	0.36	**2.76**
9-16ºC					
SAR peak isometric force (P_0)	**<0.0001**	0.1624	0.00767	1.19	0.84
SAR time to 90% P_0	**<0.0001**	**<0.0001**	-0.0314	0.49	**2.06**
SAR rate of force development	**<0.0001**	**<0.0001**	0.0390	**2.46**	0.41
SAR electromechanical delay	**<0.0001**	**<0.0001**	-0.0297	0.50	**1.98**
RCP peak isometric force (P_0)	**<0.0001**	**0.0286**	0.0076	**1.19**	0.84
RCP time to 90% P_0	**<0.0001**	**<0.0001**	-0.0268	0.54	**1.85**
RCP rate of force development	**<0.0001**	**<0.0001**	0.0345	**2.21**	0.45
RCP electromechanical delay	**<0.0001**	**<0.0001**	-0.0406	0.39	**2.54**
14-21ºC					
SAR peak isometric force (P_0)	**<0.0001**	0.8517	0.0011	1.02	0.98
SAR time to 90% P_0	**<0.0001**	**0.0073**	-0.0128	0.74	**1.34**
SAR rate of force development	**<0.0001**	0.0802	0.0139	1.38	0.73
SAR electromechanical delay	**<0.0001**	**0.0011**	-0.0224	0.60	**1.67**
RCP peak isometric force (P_0)	**<0.0001**	**0.0048**	0.0096	**1.25**	0.80
RCP time to 90% P_0	**<0.0001**	**<0.0001**	-0.0272	0.53	**1.87**
RCP rate of force development	**<0.0001**	**<0.0001**	0.0368	**2.33**	0.43
RCP electromechanical delay	**<0.0001**	**0.0003**	-0.0249	0.56	**1.78**
19-26ºC					
SAR peak isometric force (P_0)	**<0.0001**	0.1775	0.0018	1.04	0.96
SAR time to 90% P_0	**<0.0001**	**<0.0001**	-0.0234	0.58	**1.72**
SAR rate of force development	**<0.0001**	**<0.0001**	0.0253	**1.79**	0.56
SAR electromechanical delay	**<0.0001**	**0.0077**	-0.0117	0.76	**1.31**
RCP peak isometric force (P_0)	**<0.0001**	**0.0107**	-0.0092	**0.81**	1.23
RCP time to 90% P_0	**<0.0001**	**<0.0001**	-0.0144	0.72	**1.39**
RCP rate of force development	**<0.0001**	0.2296	0.0053	1.13	0.89
RCP electromechanical delay	**0.0040**	**<0.0001**	-0.0213	0.61	**1.63**

P-values are shown for individual and temperature, as in the partial regression coefficient for the temperature effect (i.e., slope) from the model from which Q_{10} values were calculated.

Bold *P*-values indicate significance levels adjusted to correct for false discovery rate (Benjamini and Hockberg, 1995). Bold Q_{10} values indicate significant temperature effects.